T.C.

TOKAT GAZİOSMANPAŞA ÜNİVERSİTESİ
LİSANSÜSTÜ EĞİTİM ENSTİTÜSÜ

MEKATRONİK MÜHENDİSLİĞİ ANA BİLİM DALI

DÜŞÜK GÜÇTE GÖMÜLÜ SABİT MIKNATISLI MOTOR TASARIMI VE UYGULAMASI

YÜKSEK LİSANS

HAMZA DIYAR

Prof. Dr. Mehmet AKAR

TOKAT – 2023

T.R.

TOKAT GAZİOSMANPAŞA UNIVERSITY

INSTITUTE OF GRADUATE STUDIES

MECHATRONICS ENGINEERING DEPARTMENT

DESIGN & APPLICATION OF LOW POWER INTERIOR PERMANENT MAGNET MOTORS

MASTER OF SCIENCE

HAMZA DIYAR

Prof. Dr. Mehmet AKAR

TOKAT – 2023

THESIS STATEMENT

I hereby declare that the rules of scientific ethics have been observed in the writing of this thesis, which has been prepared in accordance with the rules of thesis writing, that where the work of others has been used, it has been cited in accordance with scientific standards, further that the innovations and results contained in the thesis have not been repeated anywhere else, that no falsifications have been made in the data used, and that no part of the thesis has been presented as another thesis work at this or any other university.

HAMZA DIYAR

November 29, 2023

ABSTRACT

DESIGN & APPLICATION OF LOW POWER INTERIOR PERMANENT MAGNET MOTORS

HAMZA DIYAR

Master's Thesis

Advisor: Prof. Dr. Mehmet AKAR

This thesis presents the design, analysis, experimental achievement and performance of an Interior Permanent Magnet (IPM) motor for use in low power range applications. IPMs are suitable for use in household appliance motors, pumps, small electric vehicles, air compressors motor and industrial fan motors. IPMs can significantly reduce power consumption compared to alternative motor types of similar power. In this thesis, an IPM has been designed and tested for use in low power electric applications. The IPM design aims to achieve maximum torque and power density at high efficiency while keeping losses low. The three basic components of the motor design, stator, rotor and permanent magnets, are considered separately with the aim of high efficiency. In order to minimize the cogging torque and thus improve the dynamic performance of the motor, a distributed winding structure is used in the stator windings. Permanent magnets are used in the rotor to provide high torque density in IPM. The magnets used are selected from high strength materials for structural integrity. The motor performance was analyzed by Finite Element Method and the results obtained were verified with the tests performed in the experimental study. According to the results obtained, it is revealed that the IPM shows a good dynamic performance with low cogging torque at high efficiency.

2023, 86 PAGES

KEYWORDS: IPM Motor, Brushless Motors, Synchronous Motors, Efficiency, Simulation.

ÖZET

DÜŞÜK GÜÇLÜ IPM MOTOR TASARIMI VE UYGULAMASI

Hamza DIYAR

Yüskek Lisans, Mekatronik Mühendisliği Ana Bilim Dalı

Tez Danışmanı : Prof. Dr. Mehmet AKAR

Bu tez çalışmasında, düşük güç aralığı uygulamalarında kullanılmak üzere bir gömülü sabit mıknatıslı motorun (IPM) tasarımı, analizi, deneysel başarımı ve performansını sunulmaktadır. IPM'ler, ev aletleri motorlarında, pompalarda, küçük elektrikli araçlarda, hava kompresörlerde ve endüstriyel fan motorlarında kullanım için uygundur. IPM'ler, benzer güçlerdeki alternatif motor türlerine kıyasla güç tüketimini önemli ölçüde azaltabilir. Bu tez çalışmasında da özellikle düşük güçlü elektrikli uygulamalarda kullanılmak üzere bir IPM tasarımı ve testleri gerçekleştirilmiştir. IPM tasarımında kayıplar düşük seviyede tutularak yüksek verimde, maksimum tork ve güç yoğunluğu hedeflenmiştir. Motor tasarımının en temel üç bileşeni olan stator, rotor ve sabit mıknatıslar yüksek verim hedefi gözetilerek ayrı ayrı ele alınmıştır. Tutma torkunun minimize edilmesi ve bu sayede motorun dinamik performansının iyileştirilmesi amacıyla stator sargılarında dağıtılmış sargı yapısı kullanılmıştır. IPM'de yüksek tork yoğunluğu sağlamak için rotorda sabit mıknatıslar kullanılmıştır. Kullanılan mıknatıslar yapısal bütünlük açısından yüksek mukavemetli malzemeden seçilmiştir. Motor performansı sonlu elemanlar yöntemiyle analiz edilmiş ve elde edilen sonuçlar deneysel çalışmada gerçekleştirilen testlerle doğrulanmıştır. Elde edilen sonuçlara göre IPM'nin yüksek verimde düşük bit tutma torku ile iyi bir dinamik performans gösterdiği ortaya koyulmuştur.

2023, 86 SAYFA

ANAHTAR KELİMELER : Gömülü Sabit Mıknatıslı Motorlar, Fırçasız Motorlar, Senkron Motorlar, Verim, Simülasyon.

FOREWORD

It is my great pleasure to provide a foreword for this thesis, which explores an important and timely topic. My academic advisor Prof. Dr. Mehmet AKAR has done an excellent job helping me researching and analyzing the subject matter, and I am confident that the insights and conclusions presented here will be of great value to those seeking to understand the topic in greater depth.

This thesis is a testament to the hard work and dedication of the author, who has gone to great lengths to ensure that the research is comprehensive and accurate. I am confident that this work will be of great benefit to those seeking to understand the subject matter,

I would like to thank the My academic advisor Prof. Dr. Mehmet AKAR for his commitment to this project, and I wish them all the best in their future endeavors.

HAMZA DIYAR

November 29, 2023

TABLE OF CONTENTS

Pages

SYMBOLS AND ABBREVIATIONS

Symbols	Explanation
f	Frequency
η	Efficiency
T_{out}	Output Torque
P_{out}	Output Power
P_{in}	Input Power
ω_m	Angular Velocity
S_{in}	Apparent Input Power
$\cos(\varphi)$	Power Factor
Q_{in}	Input Reactive Power
η_d	Desired Efficiency
E_{ph}	Phase Back Electro Magnetic Force
f_s	Supply Frequency
N_{tph}	Number of Effective Turn per Phase
k_w	Winding Factor
φ_p	Pole Flux
P_{cu}	Copper Losses
m	Number of Phases
R_{ac}	AC Resistance
I_{ph}	Phase Current
$2p$	Pole Pairs
n	Rotation Speed
f	Operation Frequency
Hz	Hertz
E	Electric Field Strength
B	Magnetic Flux Density (intensity)
H	Magnetic Field Strength
J	Surface Current Density

D	Electric Flux Density
ρ	Electric Charge Density
μ	Permeability of Material
A	Cross-Section Area of Material
l	Length of Material
F	Magnetic Force
l_{ge}	Effective Airgap Distance
P_g	Airgap Permanence
Φ	Magnetic Flux
k_c	Carter’s Coefficient
g	Airgap Distance
Ω	Ohm
A_{rms}	Root Mean Square Amper
V_{rms}	Root Mean Square Volt
Nm	Newton Meter
dB	Decibel
$°C$	Celsius Degree

Abbreviations	**Explanation**
AC	Alternating Current
DC	Direct Current
IPM	Interior Permanent Magnet
IEC	International Electrotechnical Commission
PMSM	Permanent Magnet Synchronous Motor
SMSM	Surface Mounted Synchronous Motor
SRM	Switching Reluctance Motors
IPMSM	Interior Permanent Magnet Synchronous Motor
EMF	Electro Magnetic Force
IGBT	Isolated Gate Bipolar Transistor
PWM	Pulse Width Modulation
FEM	Finite Element Method

LIST OF FIGURES

Figure **Page**

LIST OF TABLES

Table Page

1 INTRODUCTION

Electric motors are devices that convert electrical energy into mechanical energy. They are the most common type of motor used in industrial and consumer applications. They are used to power a wide range of machines and equipment, from fans and pumps to cars and robots. Electric motors have been around since the early 19th century, when they were first developed by Michael Faraday (Helwig, 1995).

Since then, they have become increasingly sophisticated and efficient, with the development of new technologies such as brushless motors and variable speed drives. Today, electric motors are used in virtually every industry, from manufacturing to transportation.

Interior Permanent Magnet (IPM) motors were initially developed in the mid-1970s by researchers at General Electric and Siemens. Subsequent work on vehicle electrification would go on to further develop this concept in the early 2000s, with the expectation of both enhanced efficiency and improved torque delivery. By 2005, this technology had been adapted for wider use in automobiles, and for more industrial and commercial applications (Rahman, 2013).

They are most commonly used in applications requiring high efficiency, such as power tools, electric vehicles, and hybrid/electric aircraft. They are also used in heating, ventilation, and air conditioning (HVAC) systems, pumps, fans, vacuums, power chairs, compressors, and conveyor belts.

Figure 1.1 IPM motor model (Agamloh et al., 2020)

IPM motor technology is becoming increasingly popular, particularly as a means of efficient operation in electric vehicles. It is becoming a preferred choice among car manufacturers because it has a better power-to-weight ratio, higher efficiency, and much less acoustic noise than induction motors. According to a survey conducted by the market research firm Allied Market Research, the global IPM motor market was valued at approximately $16 billion in 2019 and is expected to reach $26 billion by 2027, growing at a Compound annual growth rate (CAGR) of 5.8% (Rahman et al., 2012).

The maximum rated speed and torque for an IPM motor varies depending on the motor type and model. Generally, the peak speed for IPM motors is around 3000-3500 rpm and peak torque is around 30 Nm (Takano et al., 2010).

The average efficiency for an IPM at low rpm is typically around 80-85%, while the average efficiency at higher rpm is typically around 90-95% (Tinazzi et al., 2019).

The history of induction motors dates back to the late 19th century. The first induction motor was developed by Nikola Tesla in 1888. Tesla's motor was a three-phase induction motor that used Alternating Current (AC) power. It was the first motor to use AC power and was the first practical motor to be used in industrial applications (Rahman, 2013).

In the early 20th Century, induction motors were further developed by engineers such as Charles Proteus Steinmetz and William Stanley. Steinmetz developed the first single-phase induction motor in 1905 and Stanley developed the first two-phase induction motor in 1906. (Rahman, 2013)

The induction motor quickly became the motor of choice for industrial applications due to its simplicity, reliability, and efficiency. By the 1950s, induction motors had become the standard for industrial applications (Alger & Arnold, 1976).

Today, induction motors are used in a wide variety of applications, from small household appliances to large industrial machinery. They are still the most widely used type of motor in the world.

Brushless DC (BLDC) motors have been around since the 1960s, but their use in consumer products has only become widespread in the last decade. The first BLDC motors were used in aerospace applications, such as the propulsion systems for satellites. In the 1970s, BLDC motors began to be used in more consumer applications such as computer disk drives and electric shavers (Mohanraj et al., 2022).

The development of BLDC motors was driven by the need for more efficient motors. Brushless motors have no physical brushes, which means that they have no contact between the rotor and the stator, resulting in less friction and wear. This makes them more reliable and longer lasting than brushed motors.

In the 1990s, the development of more powerful and efficient microcontrollers made it possible to control BLDC motors more precisely. This allowed them to be used in more applications, such as electric vehicles, robotics, and industrial automation (Mohanraj et al., 2022).

Today, BLDC motors are used in a wide range of applications, from consumer products to industrial machinery. They are highly efficient, reliable, and durable, making them a popular choice for many applications.

Interior Permanent Magnet Synchronous Motors (IPMSM) are a type of synchronous motor that has become increasingly popular in recent years due to their numerous advantages over traditional motors, it uses permanent magnets embedded in the rotor to create a magnetic field. This type of motor offer improved efficiency, higher power density, capable of producing high torque at low speeds and with greater controllability, making them an ideal choice for a variety of applications. IPM motors are used in a variety of applications, including electric vehicles, robotics, and industrial automation. They are also well-suited for variable speed applications, as they can be controlled with a variable frequency drive. IPM motors are more expensive than other types of motors, but their high efficiency and low maintenance requirements make them a cost-effective choice in many applications.

IPM motors are constructed with a stator and a rotor. The stator consists of a number of coils that are arranged in a specific pattern, and the rotor is made up of permanent magnets that are embedded in the rotor.

When an alternating current is applied to the stator, it creates a rotating magnetic field. This field interacts with the magnetic field of the permanent magnets in the rotor, causing it to rotate in sync with the stator. The speed of the motor is determined by the frequency of the alternating current applied to the stator.

The efficiency class of an IPM motor is typically determined by the International Electrotechnical Commission (IEC) standard 61800-9. This standard defines five different efficiency classes, ranging from IE1 to IE5. The higher the efficiency class, the more efficient the motor is. The most efficient motors are typically rated as IE4 or IE5 (Ustun & Kara, 2018a).

Synchronous motors are AC motors that run at a constant speed and are driven by AC power. They are used in a variety of applications, from industrial machinery to home appliances. Synchronous motors are typically more efficient than asynchronous motors, as they have fewer losses due to the lack of slip. They are also more reliable, as they can be designed to run at a constant speed regardless of load. Synchronous motors are also more expensive than asynchronous motors, due to their higher complexity (Sebastian et al., 1986).

The efficiency (η) of a motor is given by dividing its output power (P_{out}) by its input power (P_{in}) by using the following equation:

$$\eta = \frac{P_{out}}{P_{in}} \tag{1.1}$$

The following elements serve as the foundation for the study's goal and objective:

- ✓ To determine the factors influencing the design of IPM motors and how they influence motor performance.
- ✓ To conduct a comprehensive review of existing performance metrics and their relationship to material and/or process parameters associated with IPM motors.
- ✓ To identify driving force factors and performance trends in the design of IPM motors.
- ✓ To survey current design principles and energy efficiency tools for efficient interior permanent magnet motor designs.
- ✓ To evaluate methods for controlling torque ripple IPM motors.
- ✓ To assess the design principles for optimizing the power density of IPM motors.
- ✓ To develop the simulation and control methodologies that can improve the performance of IPM motors.

2 LITERATURE REVIEW

The first electric motor was invented by Michael Faraday in 1821. Faraday's motor was the first device to convert electrical energy into mechanical energy. It was a simple device consisting of a wire wound around a cylinder, with an electric current running through it. When the current was applied, the wire would rotate around the cylinder, creating a rotary motion. This was the first demonstration of the principle of electromagnetism, which would later be used to power a variety of devices. Faraday's motor was not very efficient, but it was a major breakthrough in the development of electric motors. It cleared the way for the development of more efficient and powerful motors that would be used in a variety of applications (Michalowicz, 1948).

Over the centuries, the field of electrical machinery has advanced to the point where it is now practically impossible to live without it. Electric vehicles and other forms of daily transportation such as scooters, buses, boats, and other vehicles are increasingly being powered by electric machines, in addition to producing electrical energy for power plants, various home appliances, and electric machines.

For example, in the enormous field of electrical machine applications, an impressive number of machines have been invented throughout human history. In the sections that follow, we will examine each type of electrical machine in turn and select those that can help reduce greenhouse gases (global warming) and store more electrical energy.

AC & DC motors are two types of electric motors that use electrical power to generate mechanical energy. AC motors generate a rotating magnetic field by using AC, whereas DC motors generate a rotating magnetic field by using direct current DC. AC motors are more efficient and can operate at higher speeds than DC motors. AC motors are also more expensive and necessitate more sophisticated controls. DC motors are less expensive and simpler, but they are less efficient and can only operate at lower speeds. AC motors are better suited to applications requiring high speeds and efficiency, whereas DC motors are better suited to applications requiring low speeds and low cost (Sakunthala et al., 2017).

The main types of motors are show in the Figure 2.1 below (Yildirim et al., 2014) :

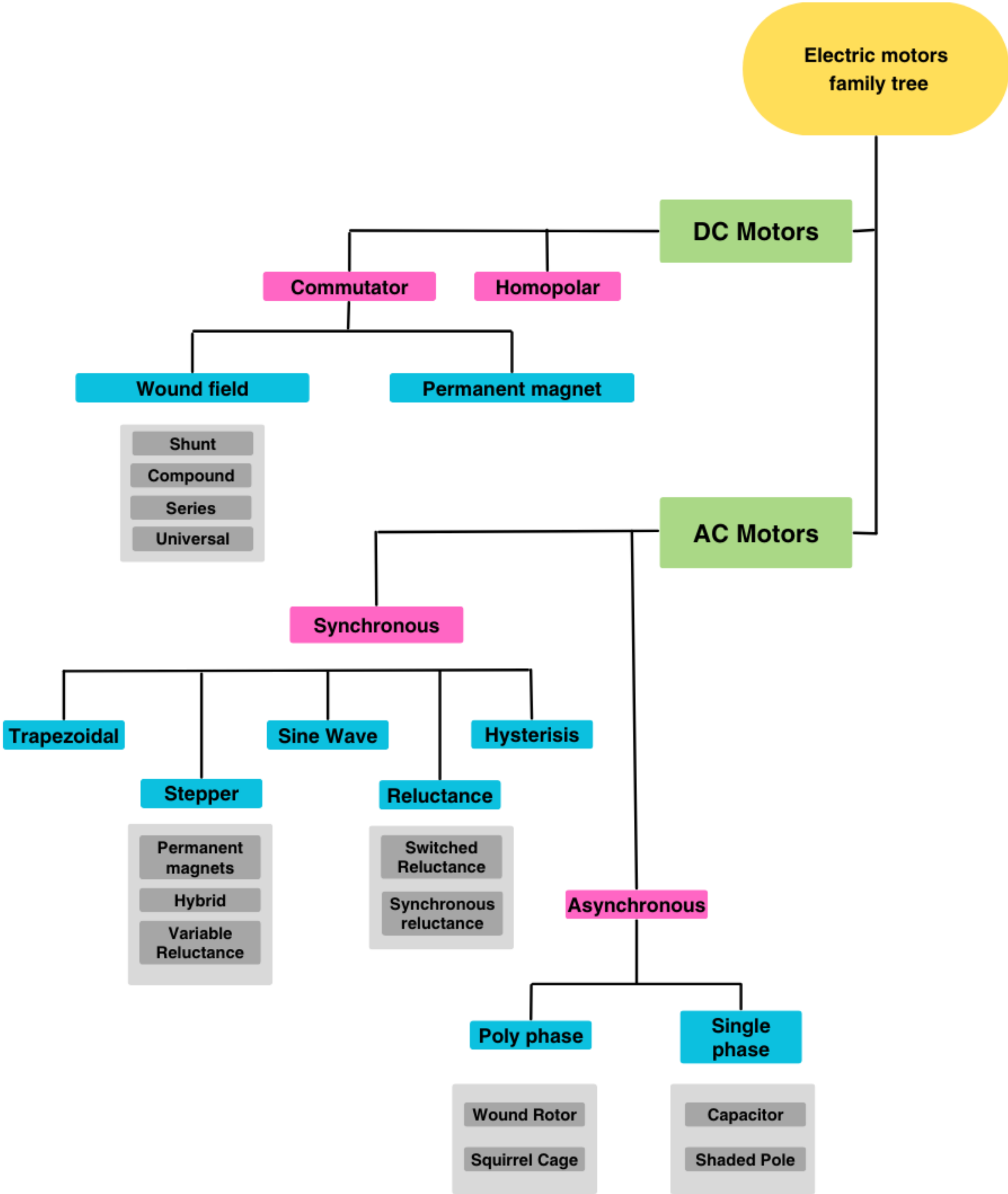

Figure 2.1 Electric motors family tree

Permanent magnet synchronous motors (PMSM)s can be broadly divided into two groups according to the placement of the magnets in their rotors as follow:

If the magnets are placed on the rotor surface, then it is a Surface Mounted Permanent Magnet Synchronous Motor (SMPMSM), and if the magnets are internally placed in the rotor, it is called Interior Permanent Magnet Synchronous Motor (IPMSM).

The Figure 2.2 shows the placement of magnets on the rotor as (a) refer to SMPMSM and (b) to IPMSM, red refer to N poles and blue for S poles.

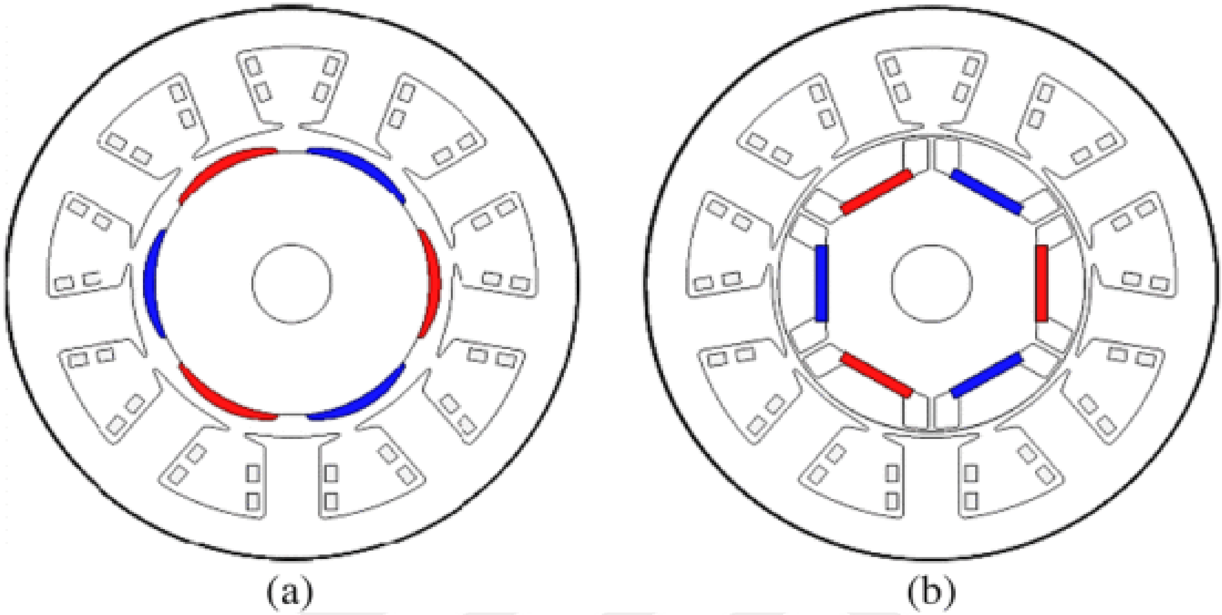

Figure 2.2 Placement of magnets on the rotor

Where Permanent Magnet (PM) motors divides into many types, main types shown below as well as in Figure 2.3:

- Surface mount (SM) PM motor
- Flux-concentrating PM motor (Spoke rotor)
- Insert PM motor
- Single-layer IPM motor
- Multi-Layer IPM motor.

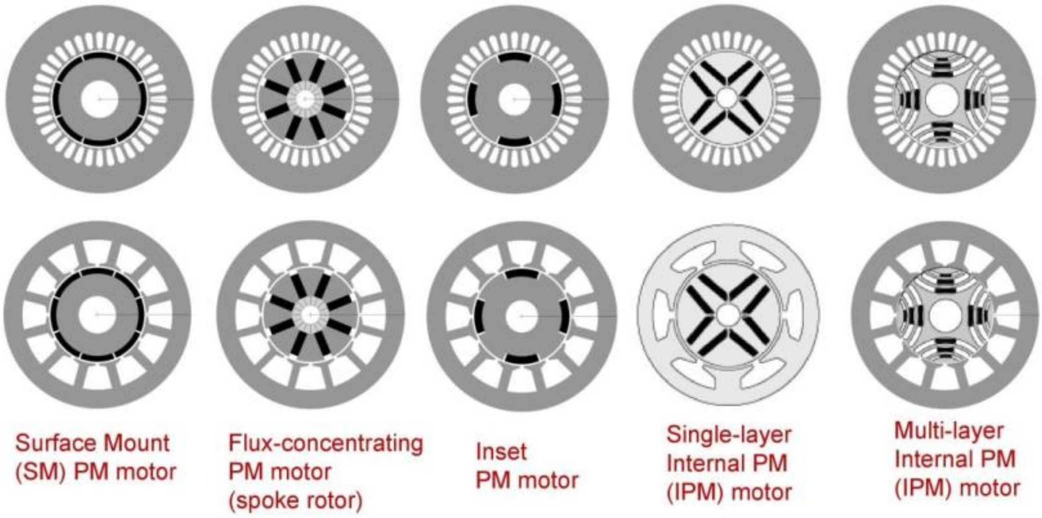

Figure 2.3 PM motors types (Zöhra & Akar, 2021)

Since the rotor of the IPMSM has saliency, there is a difference between the inductance values in d- and q-axes.

This saliency provides the generation of reluctance torque added to the torque value from the magnets, and therefore the torque capacity of the IPMSM is higher.

By accurately controlling the reluctance torque, it is possible to achieve higher torque output with lower current magnitudes (Akatsu et al., 2008).

By comparing SMPMSM and IPMSM in terms of thermal, mechanical and electromagnetic properties for high-speed applications, it has been revealed that IPMSM is superior to SMPMSM in terms of cost and that SMPMSMs have fewer heating problems (Akatsu et al., 2008).

Likewise, by comparing the loading conditions, loss rates and thermal properties of these two motor types, it has been observed that the losses increase at low speeds in IPMSMs and that the cost may increase to reduce these losses, while extra energy losses occur in SMPMSM.

The main reason for choosing AC motors is because they have less maintenance and repair requirements and it is widely used in due to its low cost and features such as durability (Akatsu et al., 2008). Where in synchronous motors, which are a group of AC motors, the rotor rotates at the magnetic field speed, this speed called synchronous speed on the other hand in asynchronous motors the rotor rotates by showing a certain amount of slip from the magnetic field inside. That is the reason behind using synchronous motors in industrial applications where constant speed is required (D. Zhang et al., 2017).

The Tables 2.1 and 2.2 below will outline the advantages and disadvantages of using PMSM. Both advantages and disadvantages must be weighed when deciding to use PMSM in any application (Li & Wang, 2016).

Table 2.1 Advantages and disadvantages of using PMSM

Advantages	Disadvantages
-The copper losses are low as it does not contain any windings in its rotor. -It does not require an external excitation current due to the presence of magnets. -Operational expenses such as maintenance and repair are eliminated due to not using the winding. -Cooling of the motor is easier since there is no winding. -It can be used safely in any environment as they do not generate arcs while working. -Since there is no brush, bracelet and collector they do not require much maintenance. This increases motor efficiency. -Their speed can be controlled within very wide limits. -Since there is no winding in its rotor, it is lighter than other motors of the same power and has a low moment of inertia.	-Since it contains magnets instead of windings, it is more costly than other motor types. -Magnetic materials have thermal constraints. -The magnetism of the magnets may decrease over time. -Magnets have a risk of demagnetization and affect the safety of the system. -When maintenance is performed by separating the rotor from the stator, there may be slippage in the operating point. -Since the stator field and the rotor field must be synchronized, they require precise rotor position information. -The position sensor used for rotor position information increases the cost. -They need external power electronics circuits as they cannot start directly.

Table 2.1 Advantages and disadvantages of using PMSM (Continue)

-The response is faster as the low moment of inertia. In other words, the ratio of torque to moment of inertia is higher in these motors. -Efficiency and power factor are better than asynchronous motors.	-In case of poor quality of permanent magnets, the performance characteristics of the motor deteriorate. -In SMPMSMs, there is a risk that permanent magnets will break at very high speeds.

Table 2.2 Comparison between different kinds of electric motors

Features	**DC Motors**	**IM**	**SRM**	**PMSM**
Cost	Average	Low	Average	High
Efficiency	Low	Good	Good	Hight
Control Method	Simple	Medium	Complex	Moderate
Durability	Short life	Last long	Last long	Medium
Power Density	Very low	Medium	Medium	Very high

In SMPM motor structures, the permanent magnets are mounted on the rotor surface by using special adhesives. One of the biggest problems encountered in this type of design is that at high speeds, centrifugal forces can overcome the adhesive force and remove the magnets from their slots. If so, it can hit the stator and get stuck in the air gap. It can cause serious mechanical damage both in the body and in the stator winding and lamination. For this reason, surface-mounted magnet designs are less preferred in applications requiring high speed (Choi et al., 2022; Niu & Chen, 2022).

IPM motors, are a type of brushless DC motor. They are typically used in applications that require high efficiency, high torque, and low speed. These motors are more efficient than traditional induction motors, and they have a higher power density. IPM motors also have a higher power factor, which means they can draw more power from the same amount of electricity (Ustun & Kara, 2018b).

What makes IPM motors so useful in electric vehicles is their high torque, which is generated by using permanent magnets around a static cylinder containing electromagnetic windings. The arrangement of these magnets and windings creates rotor motion when current is applied to the windings, which is used to create torque and power. The high torque output of IPM motors makes them particularly useful for electric vehicles, as they can provide a high level of performance while keeping the weight and size to a minimum. This often results in a lighter and more efficient electric vehicle, as the weight and size of the motor can be reduced without harming the performance of the vehicle. This makes them ideal for use in electric vehicles such as cars, buses, and scooters.

Additionally, the high torque output makes IPM motors suitable for use in electric vehicles in high life-cycle applications, such as in electric buses and delivery trucks, which are required to drive long-distances often. In these applications, the high torque output can make it easier for the vehicle to ascend steep gradients without the need for additional power sources (Gudivada et al., 2017).

Finally, the advanced control capabilities of IPM motors make them suitable for use in electric vehicles which require precise control, such as electric supercars and commercial electric vehicles. With these motors, drivers can adjust the output of the motor depending on the conditions, allowing for improved traction and acceleration.

Overall, the use of IPM motors in electric vehicles has many advantages, such as high torque output, low weight, and the ability to handle high life-cycle applications. This makes them an attractive option for those looking to build electric vehicles, as they can provide a light and efficient motor that can handle high levels of performance (Wang et al., 2018).

3 MATERIALS AND METHODS

Materials used in the design of a IPMSM include high-grade electrical steel sheets, magnets, copper windings, an insulated coating, and a ventilated external case. Depending on the application, the particular type of material used may vary. For example, the copper windings could be either an aluminum or copper alloy, or may contain a superconductive material. The insulation coating could be a dielectric or insulating film. The external case needs to be ventilated for cooling purposes, which is an important factor affecting performance and life.

The assembly and manufacturing processes used for the IPMSM vary in complexity and precision. For example, manual winding can be used, or a winding machine may be used instead for faster and more consistent results. The magnets are usually hand-placed in the rotor, while the electrical connection in the stator needs to be accurate and well-insulated. Furthermore, the assembly should be carried out in a dust-free environment.

3.1 IPM Design Process

The design process of an electrical motor involves several steps and considerations, such as selecting a type of motor, designing the motor's various components, specifying its performance characteristics, and building a prototype as cleared in figure 3.1. The choice of motor type depends on the application, as various motors deliver different levels of efficiency, air gap flux density and harmonics, cogging torque, Back-EMF waveforms, generated torque, torque speed curves, torque ripples, magnet demagnetization analysis, mechanical stress analysis, and radial force analysis, and output power. The components of an electrical motor, such as the stator, rotor windings, and bearings, are then designed according to the requirements of the application. The motor's performance characteristics are closely related to the components, and must meet the specific needs of the system. Finally, a prototype motor is built and tested to ensure it meets all requirements. Advanced motor designs can often involve computer modelling, to optimize the performance of its components (An et al., 2016).

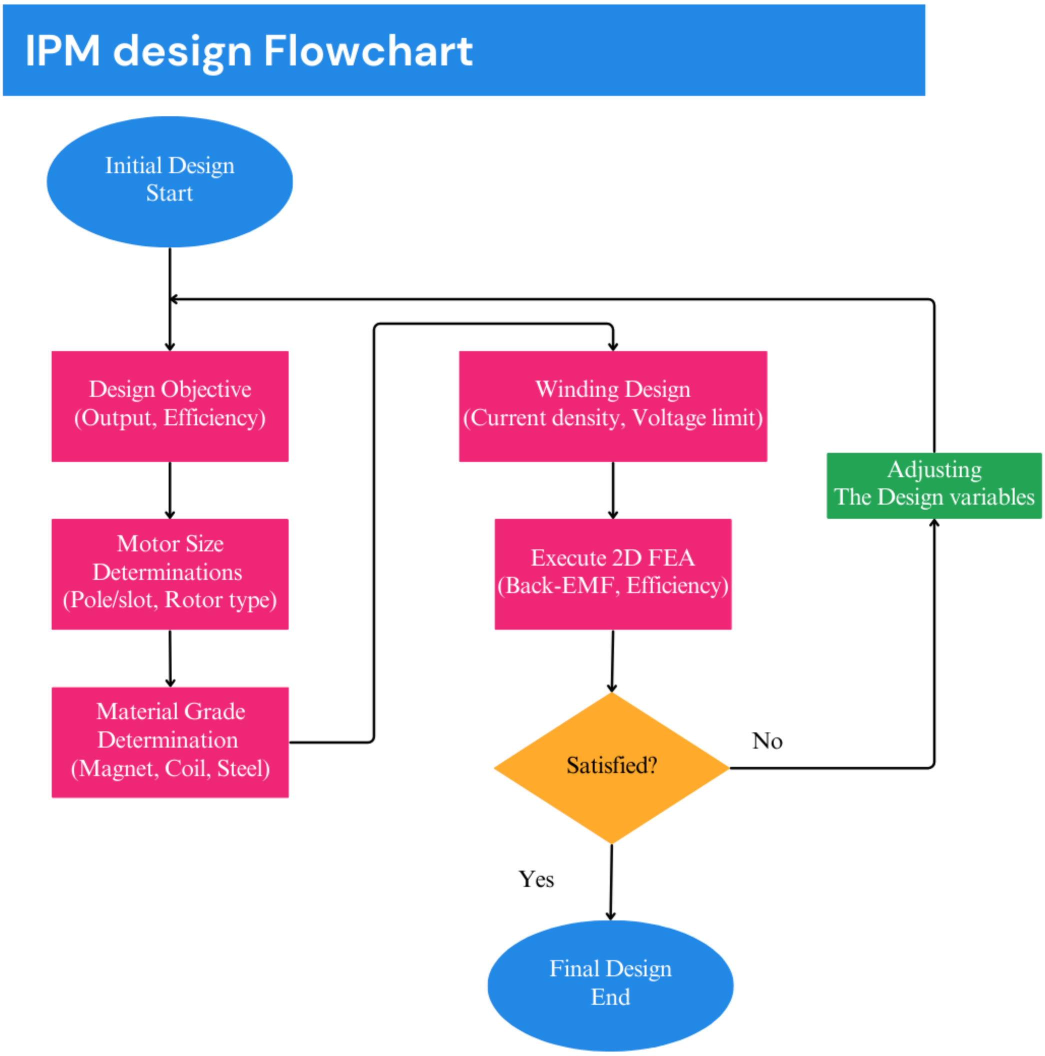

Figure 3.1 IPM design flowchart (Yoon & Baek, 2020)

The design of electrical motors plays a critical role in the performance of the system output torque. The design of the electrical motor determines the amount of torque that can be generated from the system. Proper design of the motor can lead to a more efficient system and increased output torque. Certain design elements such as reinforcement laminates and heat sinks can prevent problems such as overheating and arcing that can drastically reduce output torque. Furthermore, poor design of electrical motors can result in costly repairs or maintenance, along with potential product damage or poor efficiency. Therefore, it is essential to understand the design of an electrical motor in order to ensure optimal performance and output torque.

The output power and output torque of an electrical motor are directly correlated, with one influencing the other. Output power is the result of output voltage and output current, whereas output torque is the result of mechanical speed and output force. An increase in output power is often reflected in an increase in output torque as long as the mechanical speed is kept constant. A greater output power will also increase the mechanical speed, but a decrease in torque will usually occurs. Therefore, when designing an electrical motor, it is essential to consider the relationship between output power, output torque, and mechanical speed in order to optimize the overall efficiency of the system.

The voltage and current components in stationary reference frame, denoted by $v_{\alpha\beta}$ and $i_{\alpha\beta}$ as shown in equation 3.1, have no filters applied to them; these values are obtained from the electrical angle with a corresponding electrical cycle (period) of time. To calculate the input electrical power is given by Equation 3.1 as follow: (Bojoi et al., n.d., 2023)

$$P_e = \frac{3}{2} \times \frac{1}{T} \int_0^T \left(v_\alpha i_\alpha + v_\beta i_\beta\right) dt \quad (3.1)$$

Where P_e refer to input electrical power, vαβ and iαβ are the current and voltage and T to the electrical cycle.

Calculating the mechanical shaft output power for electric motors is very important for ensuring their desired efficiency is achieved. This calculation is done using Equation 3.2, 3.3 and 3.4 involving the motor's output torque, speed, and efficiency.

$$P_m = T_m \times \omega_m \quad (3.2)$$

$$T_{out} = \frac{P_{out}}{\omega_m} \quad (3.3)$$

$$\omega_m = 2\pi \times \frac{rpm}{60} \quad (3.4)$$

Where T_m refer to measured torque, T_{out} rated output torque, P_{out} rated output power and ω_m to rated angular velocity.

$$P_{in} = \frac{P_{out}}{\eta_d} \quad (3.5)$$

$$S_{in} = \frac{P_{out}}{\eta_d \times \cos(\varphi)} \quad (3.6)$$

$$Q_{in} = S_{in} \times \sqrt{1 - \cos(\varphi)^2} \quad (3.7)$$

Where P_{in} refer to Input real power, η_d Desired efficiency, S_{in} Input apparent power, $\cos(\varphi)$ Desired power factor and Q_{in} Input reactive power.

Using those equations helps to ensure that the desired efficiency is achieved from the motor, making it important for understanding how much power needs to be put into the motor for a desired output.

The phase Back EMF is the voltage induced in the rotor as the current passes through the stator winding. It is proportional to the rotor speed and can be calculated using various mathematical formulas. However, it can also be measured using an oscilloscope or an electrometer. The phase Back EMF is a critical factor when determining the power factor of an electric motor and its efficiency. The phase back emf can be calculated using the Equation 3.8 as following:

$$E_{ph} = 4.44 \times f_s \times N_{tph} \times k_w \times \varphi_p \tag{3.8}$$

Where f_s refer to rated frequency of supply, N_{tph} number of effective turns per phase, k_w winding factor and φ_p pole flux.

Total losses include losses due to heat generated by winding resistance, stray losses due to eddy current and hysteresis and mechanical losses due to friction and windage. Specific losses include Joule heating due to winding losses, winding skin effect losses, core losses due to hysteresis and eddy currents, rotating losses due to bearing friction, windage, and ventilation losses. Accurate calculation of losses in motors not only ensures proper motor design but also enhances motor efficiency.

Figure 3.2 Total losses in electric motors

Copper losses are generated in the electrical wiring of the motor as a consequence of the flow of current. The higher the current, the more energy is dissipated as heat as the current moves through the copper wire. The larger the motor, the greater the amount of wiring and the more heat is generated. The temperature also affects how much energy is lost in the copper wiring. Larger motors require more careful calculations of the copper losses to ensure optimal performance (Bojoi et al., n.d., 2023).

$$P_j = R_{s,avg} \frac{1}{T}\int_0^T (i_a^2+i_b^2+i_c^2)\, dt \tag{3.9}$$

$$P_{cu} = mR_{AC} \times I_{ph}^2 \tag{3.10}$$

Where m refer to number of phases, R_{AC} to AC resistance, I_{ph}^2 to phase current, P_j to joule losses and $R_{s,avg}$ to the average stator resistance (Caruso et al., 2017).

3.1.1. Selection of the number of poles

The number of poles in PM machines is based on the rotor speed, which is the main determining factor in the design. For the same speed value, increasing in the number of poles causes increases in the commutation frequency, thus an increase in the switching losses of the switching elements and an increase in the iron losses of the stator core (X. Zhang & Qu, 2013).

Advantages and disadvantages of increasing the number of poles are listed in the Table 3.1:

Table 3.1 Advantages and disadvantages of increasing the number of poles

Advantages	**Disadvantages**
Reduction in the cross sections of active materials	The number of pole pairs directly affects flux leakage
Increased pole numbers lower magnet costs	Iron losses increase as the number of pole pairs increases
With the same stator diameter, a greater rotor diameter is possible	Need for higher PWM frequencies for more poles
With the same rotor, the stator diameter can be reduced.	
Efficiency increases as phase resistance decreases due to shorter coil lengths	

The chosen number of poles is given as the following Equations 3.11, 3.12 and 3.13:

$$2p = 120 \times \frac{f}{n} \tag{3.11}$$

$$2p = 120 \times \frac{250}{3000} \tag{3.12}$$

$$2p = 10 \tag{3.13}$$

Where $2p$ refer to poles number, f operation frequency and n rotation speed

3.1.2. Motor calculations

The efficiency of the motor with a rated power of 0.8 kW has been obtained as ~ 88% under full load operation in the ANSYS Maxwell RmXprt Software

According to that;

$$\text{Rotation speed} = \frac{120*f}{2p} \tag{3.14}$$

Where the rated rotation speed is 3000 rpm and $2p$ is 10 so we can calculate the operating frequency according to the Equation 3.15 as following:

$$rpm = \frac{120*f}{2p} \tag{3.15}$$

$$f = 250\,Hz$$

3.1.3. Motor parameters

The following table outlines the essential parameters of an electrical motor which are required to evaluate its suitability for a given application. These parameters include power rating, efficiency, speed, torque output, and other such critical specifications. This information can be used to assess the motor’s performance when operating under various conditions as well as to size a motor for specific power and torque requirements. Additionally, understanding the parameters allows for further comparison between different motors to select the most appropriate one.

Table 3.2 General parameters

Rated output power	0.8 KW
Rated voltage	220 V
Rated speed	3000 rpm
Operation frequency	250 Hz

Table 3.3 Stator parameters

<table>
<tr><td>Number of poles</td><td colspan="2">10</td></tr>
<tr><td>Number of slots</td><td colspan="2">12</td></tr>
<tr><td>Outer diameter</td><td colspan="2">120 mm</td></tr>
<tr><td>Inner diameter</td><td colspan="2">79.95 mm</td></tr>
<tr><td>Length</td><td colspan="2">40 mm</td></tr>
<tr><td>Stacking factor</td><td colspan="2">0.95</td></tr>
<tr><td>Steel type</td><td colspan="2">JFE Steel 35JN440</td></tr>
<tr><td rowspan="6">Slot geometry
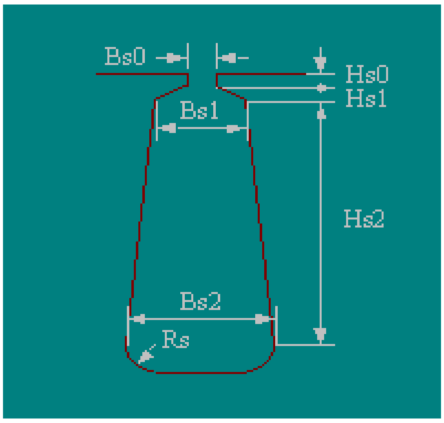

Figure 3.3 Slot geometry</td><td>Tooth width</td><td>10.5 mm (Parallel)</td></tr>
<tr><td>Hs0</td><td>1.5 mm</td></tr>
<tr><td>Hs1</td><td>1 mm</td></tr>
<tr><td>Hs2</td><td>12 mm</td></tr>
<tr><td>Bs0</td><td>2 mm</td></tr>
<tr><td>Rs</td><td>1.5 mm</td></tr>
<tr><td>Winding layers</td><td colspan="2">2</td></tr>
<tr><td>Winding type</td><td colspan="2">Star (Y) Whole-Coiled</td></tr>
<tr><td>Parallel branches</td><td colspan="2">1</td></tr>
<tr><td>Conductor per slot</td><td colspan="2">80</td></tr>
<tr><td>Coil pitch</td><td colspan="2">1</td></tr>
<tr><td>Number of strands</td><td colspan="2">3</td></tr>
</table>

Table 3.4 Stator parameters (Continue)

Wire wrap mm	0.04
Wire size (Ø) mm	0.51
Conductor type	Copper

Table 3.5 Rotor parameters

<table>
<tr><td>Outer diameter</td><td colspan="2">73.95 mm</td></tr>
<tr><td>Inner diameter</td><td colspan="2">15 mm</td></tr>
<tr><td>Length</td><td colspan="2">40 mm</td></tr>
<tr><td>Stacking factor</td><td colspan="2">0.95</td></tr>
<tr><td>Steel type</td><td colspan="2">JFE Steel 35JN440</td></tr>
<tr><td rowspan="6">Geometry
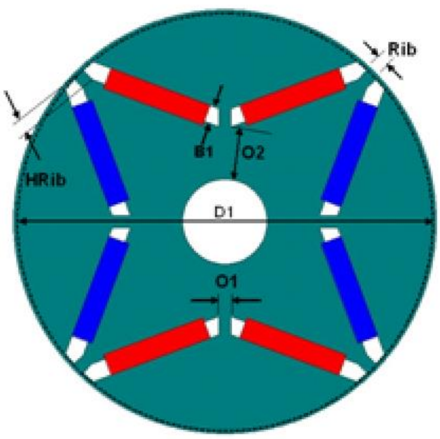

Figure 3.4 Rotor parameters</td><td>D1</td><td>72.95 mm</td></tr>
<tr><td>O1</td><td>0.6 mm</td></tr>
<tr><td>O2</td><td>10 mm</td></tr>
<tr><td>B1</td><td>3.1 mm</td></tr>
<tr><td>Rib</td><td>0.5 mm</td></tr>
<tr><td>HRib</td><td>0.5 mm</td></tr>
<tr><td>Magnet thickness</td><td colspan="2">3 mm</td></tr>
<tr><td>Magnet width</td><td colspan="2">28 mm</td></tr>
<tr><td>Magnet type</td><td colspan="2">NdFe35</td></tr>
</table>

3.1.4. Finite elements method

The finite element method (FEM) was first used in structural analysis. Semi-analytical analysis methods were developed by Hrennikoff (1941) and Mc Henry (1943). In the 1960s and 1970s, the FEM was used to analyze twisted plane surfaces and three-dimensional pressure vessels. It has been widely used in structural, fluid and thermal analysis of problems (Okur, 2007).

FEM is currently the most preferred numerical method for solving complex engineering problems. The reason why the method is frequently used in engineering fields is that only the input for solving any particular problem by varying the parameters can be used. The main goal of FEM is to find a solution to a complex problem by simplifying it. By reducing the problem to a simpler problem, an approximate result is obtained instead of an exact result. In complex mathematical equations, FEM is the only method that can be used if there is no exact result or even an approximate result (Akgün G., 2013).

FEM is frequently preferred in the analysis of magnetic fields, performance calculations of electrical machines, solution of thermal and hydraulic problems, bending, torsion and fracture analysis, mechanical strength and force calculations. The foundations of electric machines are based on the principle of interacting with the electromagnetic field. In other words, electromagnetic phenomena can be expressed in the mathematical form of Maxwell's electromagnetic equations. Maxwell's equations can be solved by analytical or numerical methods. Analytical methods can be used to model equivalent circuits and finite element methods can be used to model electrical machines and complex geometries (Dönmezer, 2009).

In order for the electric machine to be produced correctly, the magnetic field analysis made during its design must be done correctly. In addition, the machine characteristics must also be calculated correctly. The magnetic materials used in the calculation of motor values in BLDCs are sloppy, complex geometry and nonlinear, making the calculation of motor values difficult along with the magnetic field analysis. In order to facilitate the solution of values and complex differential equations, FEM is one of the most preferred mathematical methods (Turhan, 2014).

The electromagnetic torque, which allows the rotation of electric machines is produced by the effect of magnetic field (Ge, 2014). Therefore, the magnetic flux of the motor distribution in the air gap needs to be accurately calculated.

Electromagnetic phenomena are comprehensively described by Maxwell's equations. can be explained. The electromagnetic field that can be described by writing a set of field equations, it can basically be expressed in terms of five vectors and one scalar (Pyrhnen, 2008). These are;

- Electric field strength, E

- Magnetic field strength, H

- Electric flux density, D

- Magnetic flux density, B

- Surface Current Density, J

- Electric charge density, ρ

The existence of an electric magnetic field implies that the magnetic field can be applied to a charged body or a current-carrying is explained by the force it exerts on a conductor. This force is created by the magnetic field effect. The force can be calculated with the Lorentz force equation. Lorentz force vector can be expressed by Equation 3.16 for a load dQ moving with velocity υ (Pyrhnen, 2008).

$$dF = dQ(E + \upsilon \times B) = dQE + \frac{dQ}{dt}dl \times B = dQE + idl \times B \tag{3.16}$$

Torque in electric machines is generated by this principle where last part of the equation is formulated with reference to a current carrying conductor of length dl.

The flow chart diagram of the finite element method is illustrating most of the post-process steps: defining the material properties, creating the FEA mesh, defining the boundary conditions and creating the model's geometry as shown in figure 3.5:

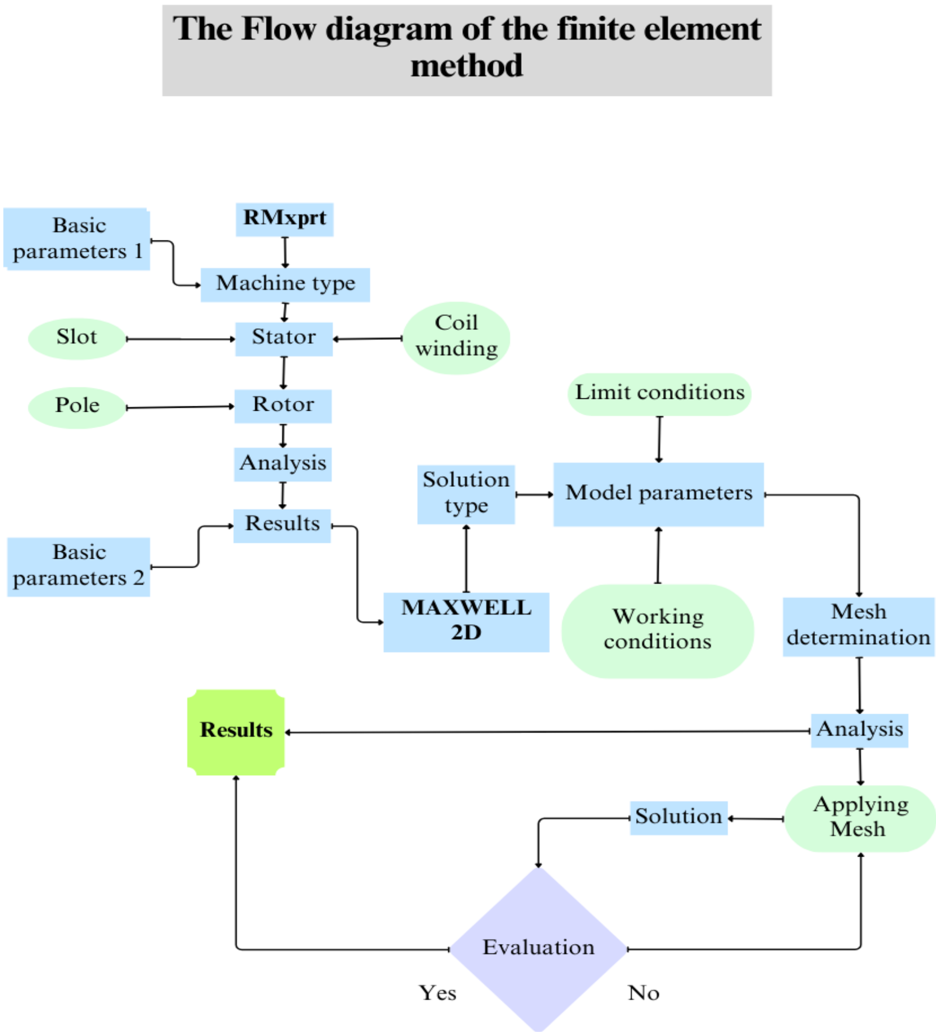

Figure 3.5 The flow diagram of FEM (K. Chari, 1974)

Using FEM, armature reaction, winding inductance, iron losses, interaction moment in brushless motors can be calculated very quickly and with approximate results.

With ANSYS Electronics program, after the meshing process, as shown in Figure 3.6 the number of regions formed called finite element number. The higher the number of meshes formed, the higher the accuracy of the analysis. However, the increase in the number of finite elements, prolongs the solution time. To improve the time and facilitate the solution, the number of finite elements could be decreased but that can lead to decrease the accuracy of the solution result (K. Chari, 1974).

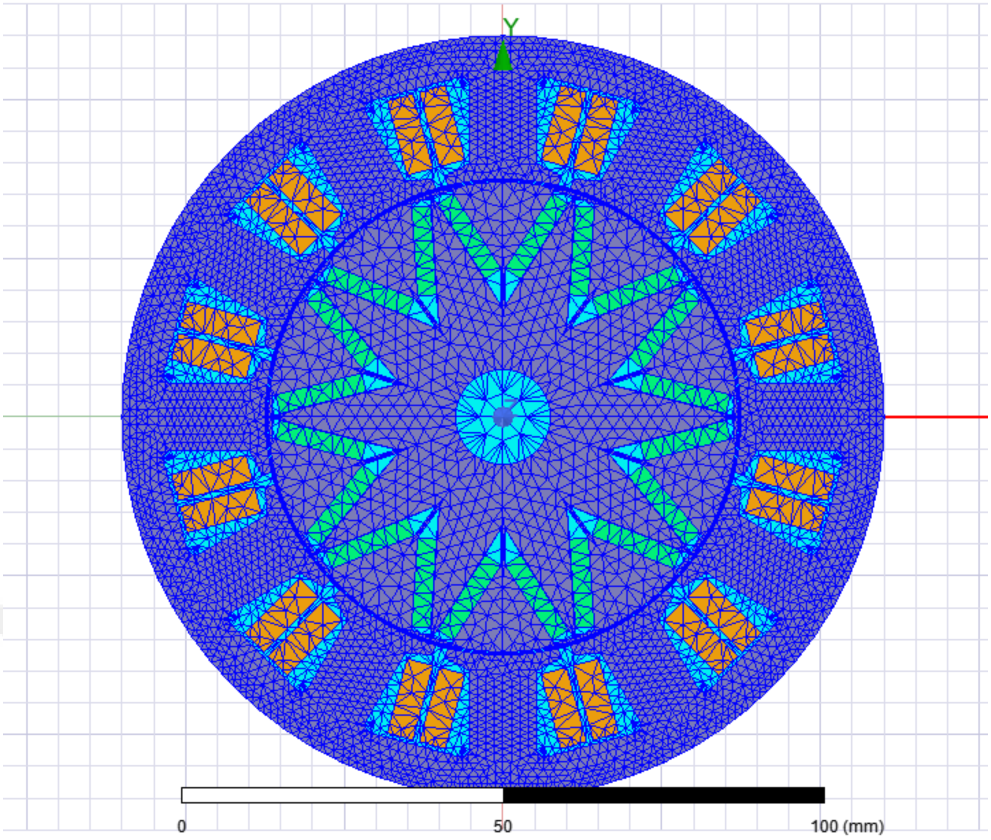

Figure 3.6 Mesh solve

3.1.5. Maxwell's equations

Maxwell's equations are a set of four equations that describe the behavior of electric and magnetic fields. The equations describe how electric and magnetic fields interact with each other and with matter. They form the basis of classical electromagnetism. The Equations 3.17, 3.18, 3.19 and 3.20 also provide insight into the behavior of light and other electromagnetic radiation.

$$\nabla \times E = -\frac{\partial B}{\partial t} \tag{3.17}$$

$$\nabla \cdot B = 0 \tag{3.18}$$

$$\nabla \times H = j + \frac{\partial D}{\partial t} \tag{3.19}$$

$$\nabla \cdot D = \rho \tag{3.20}$$

Where E refer to electric field strength in V/M, B magnetic flux density in Wb/m^2, H magnetic field strength in A/m, J surface current density in A/m^2, D magnetic flux density in C/m^2, and ρ volume charge density in C/m^3.

The properties of the macroscopic material can be given by the equations shown in the Equations 3.21, 3.22 and 3.23:

$$j = \sigma E \tag{3.21}$$

$$D = \varepsilon E = \varepsilon_0 \varepsilon_r \tag{3.22}$$

$$B = \mu H = \mu_0 \mu_r H \tag{3.23}$$

Where σ electrical conductivity, $\varepsilon_0 \varepsilon_r$ electrical permeability, μ magnetic permeability, μ_0 permeability of the air and μ_r magnetic relative permeability

3.1.6. Torque and magnetic energy equations

Formulating the mathematical method for the motor will be required in order to compute the torque and magnetic energy. The magnetic field distribution within the motor is essential here since it has a direct influence on magnetic energy. A magnetic field is described by two vector quantities: flux density B and field strength H. The Equation 3.24 describes the relation between B and H:

$$B = \mu \times H \tag{3.24}$$

where μ refer to permeability of the material.

Magnetic flux is the flux density that travels through a certain area. It is written as shown in the Equation 3.25 below:

$$\Phi = B \times A \tag{3.25}$$

where A refer to the cross-sectional area of the material.

The total differences in the magnetic field intensity according to distance is known as magnetomotive force. As described in the Equation 3.26:

$$F = H \times l \tag{3.26}$$

Where l is the length of the material.

The magnetic permeance is given by the ratio of Φ and F given by the Equation 3.27:

$$P = \frac{\mu \times A}{l} \quad (3.27)$$

Until this section the basic equations have been explained so far. Now it is important to use those equations to explain other magnetic relationship. In all motors flux travels through the air gap between the rotor and stator. As a result, the permeance or reluctance of the air gap should be modeled properly. The formula in the Equation 3.28 can be used to compute air gap permeance:

$$Pg = (\mu 0) \times (AlgeP_g = (\mu_0) \times (\frac{A}{lg_e}) \quad (3.28)$$

where lg_e is the effective air gap distance. As it shows in 3.29;

$$lg_e = K_c \times lg \quad (3.29)$$

where K_c is the Carter's coefficient and lg is the air gap distance. In the case of an armature with open or semi-enclosed slots, the Carter's coefficient is a value that can be used to determine the effective or contracted slot pitch. The parameter K_c is provided as 3.30:

$$K_c = [1 - \frac{1}{\frac{\tau_s}{\omega_s} \times \left(\frac{5 \times lg}{\omega_s} + 1\right)}]^{-1} \quad (3.30)$$

3.1.7. Motor solving

The ANSYS program is a PC platforms finite element package program. Finite element analysis for a physical object is explained in the following steps:

- Mathematical model of the system
- Placing finite elements on the model
- Determination of material properties
- Resource identification
- Determination of boundary conditions
- Determining the elements of the equations according to the finite elements and bringing them into matrix form
- Solving equations of unknown variables
- Results of analysis

After entering the parameters into the simulation program, the analytical model of the motor is created and the design stages are carried out as in Figure 3.7. Then, after the model is created in RMxprt mode, the necessary steps for analytical modeling are made and modeling work is done.

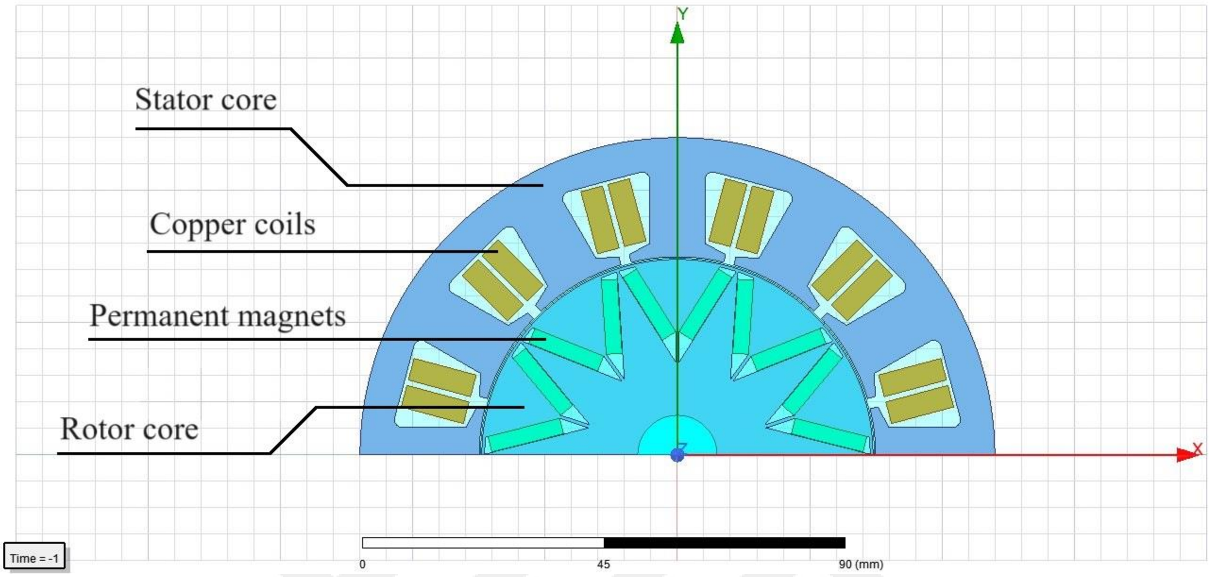

Figure 3.7 Analytical model of the motor

Magnetic flux density is a measure of how much total magnetic flux there is in a given area. It is the magnetic flux per unit area, usually measured in Tesla (T). It is also referred as "magnetic field density," "magnetic field strength," or "magnetic induction."

Magnetic flux density is an important property that influences performance. It is the amount of total magnetic field that is generated inside the motor, which is determined by the magnetic circuit design and the surrounding material properties. Magnetic flux density determines the motor's torque, efficiency, and power output (Sahin, 2001).

For electric motor design, the magnetic flux density of the motor should be considered as well as the local environment. The shape and size of the motor's magnetic circuit as well as the amount of ferromagnetic material in the vicinity of the motor need to be taken into consideration. The local ambient magnetic field and other magnetic fields in the vicinity of the motor also should be considered (Ge, 2014).

It is desirable to have a high magnetic flux density in order to achieve a high torque output. However, the saturation of the magnetic material will limit the attainable flux density. Too much flux density may lead to core losses, which will degrade the motor efficiency. Too little flux density can cause insufficient torque output.

Therefore, the magnetic circuit of an electric motor must be carefully designed in order to achieve the desired magnetic flux density. This includes optimizing the dimensions of the magnetic circuit, material selection, and positioning of components relative to each other. By doing this, the magnetic flux density of the motor can be accurately determined and optimized for improved performance (Dönmezer, 2009).

In the Figure 3.8, Magnetic flux density is shown and measured where the maximum value reached shown in red and the minimum value shown in blue which is in the limits of safe operation.

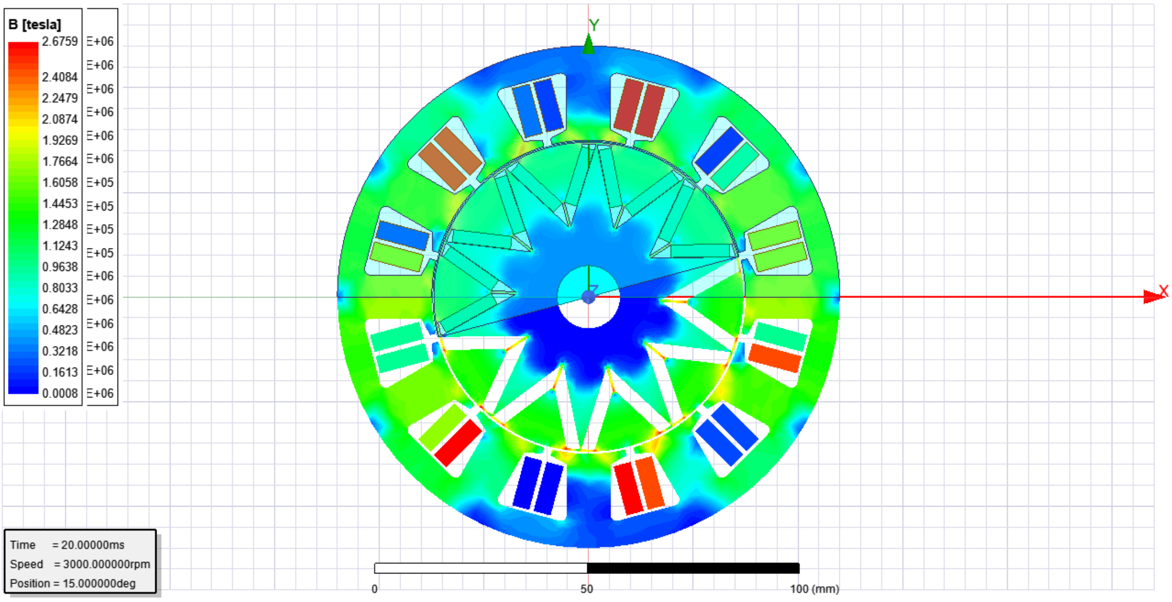

Figure 3.8 Magnetic flux density of the motor

3.1.8. 3D Design

The 3D model designed on SolidWorks is a highly-detailed and realistic representation of a product. This model was created using the features and tools offered by the software, giving it the capabilities to create realistic designs without sacrificing quality. The software shows intricate details and a high level of accuracy to the exact specifications in the virtual environment. This detailed model figures 3.9, 3.10 and 3.11 also allows us to assess the functionality, strengths, weaknesses and exploded view of the product.

Figure 3.9 Motor 3D housing Design

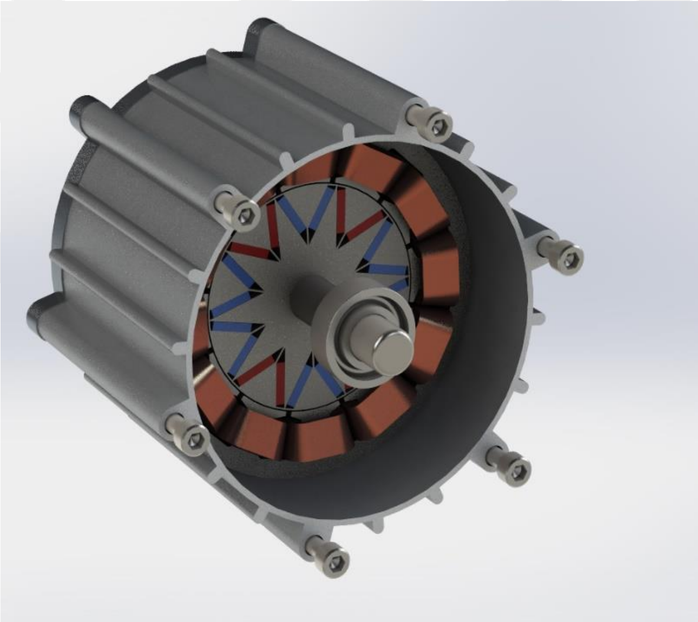

Figure 3.10 3D Design of the motor

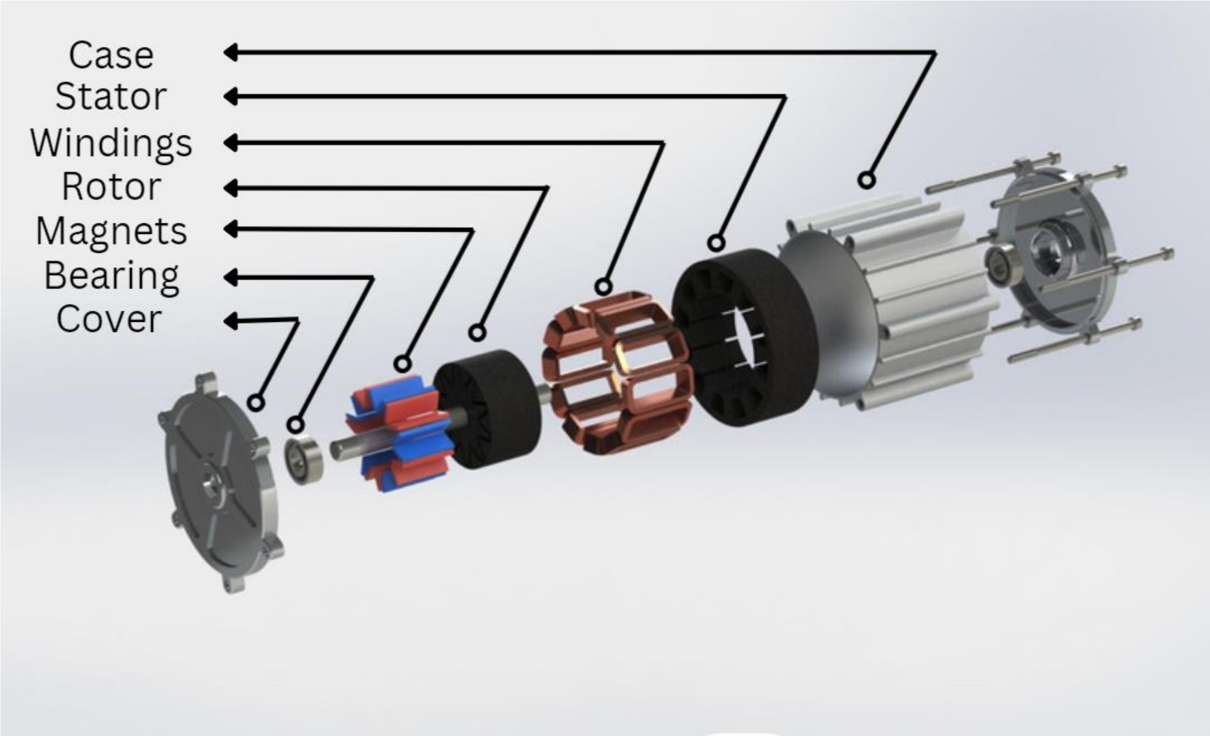

Figure 3.11 Exploded 3D view of the motor

3.2. Mathematical Models

It is essential to understand the dynamic and mathematical machine model as well as its electrical and magnetic properties in order to study the electric and magnetic behavior of the IPMSM under various operating situations. Traditional dynamic and mathematical machine models are discussed in literature. The standard dynamic and mathematical IPMSM model's fundamental simplifying hypotheses are as follows:

- The magnetomotive force's sinusoidal distribution of space in the air gap.

- The machine's linear magnetic behavior.

- The iron core has no hysteresis or eddy currents.

- No cross coupling effects.

- No impacts of slot harmonics.

- The machine is affected by an insufficient amount of heat.

The general voltage formulas are as in Equations 3.31, 3.32 and 3.33 when referring to a three-phase IPMSM:

$$v_a = Ri_a(t) + \frac{d\lambda_a(t,\theta_e)}{dt} \tag{3.31}$$

$$v_b = Ri_b(t) + \frac{d\lambda_b(t,\theta_e)}{dt} \tag{3.32}$$

$$v_c = Ri_c(t) + \frac{d\lambda_c(t,\theta_e)}{dt} \tag{3.33}$$

Where v_a, v_b and v_c refer to the instant phase voltages, i_a, i_b and i_c to the instant phase currents, λ_a, λ_b and λ_c to the instant magnetic phase flux linkage, θ_e refer to the rotor electrical position and R for the phase resistance (Caruso et al., 2017).

According to the dq0 synchronous reference structure, the IPMSM mathematical model:

Three differential equations with variable coefficients define the mathematical model in the stator reference structure system as mentioned before. It can be hard to apply forward the use of such a mathematical model for the purpose of operating an IPMSM. Linear mathematical transformations can be applied to create differential equations with constant parameters. In particular, Park transformation enables the change from a three-phase stator reference system to a two-phase reference structure system, with the real axis coincident with the polar rotor axis and revolving at the electrical rotor angular speed ω_r.

This transformation has the advantage of being simplified to a set of equations in the reference (dq0), where the self- and mutual induction coefficients are independent of the rotor location and remain constant across time. As revealed in Figure 3.12, the stator reference system (a,b,c) is transformed to the fixed two-phase reference system (α, β) in order to produce the Park model.

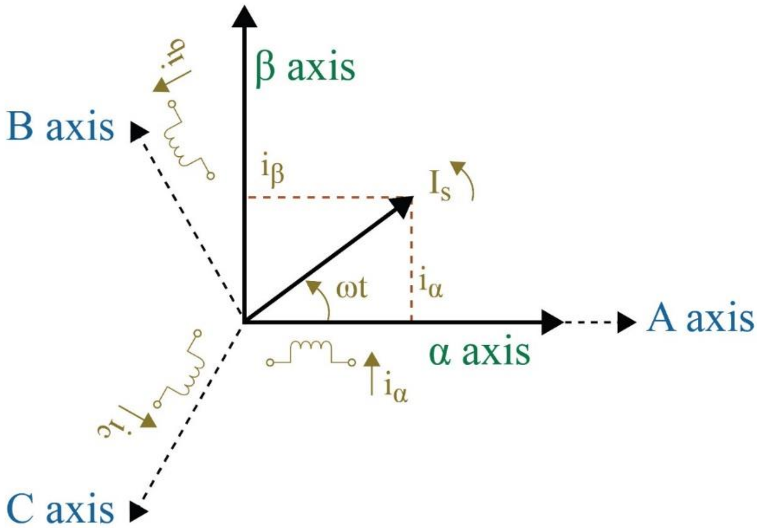

Figure 3.12 (a,b,c) reference system is transformed to the fixed two-phase reference system (α,β)

The expression of electromechanical torque consists of two parts: the fundamental torque, which depends on the flux linkage created by permanent magnets and q-axis current, and the reluctance torque, which depends on the saliency of the machine and both d- and q-axis currents. The mechanical balancing Equations 3.34, 3.35 and 3.36 from the IPMSM conventional dynamic and mathematical model are provided as follow:

$$v_d = Ri_d + L_d \frac{di_d}{dt} - \omega_e L_q i_q \qquad (3.34)$$

$$v_q = Ri_q + L_q \frac{di_q}{dt} + p\omega_e L_d i_d + \omega_e \lambda_{PM} \qquad (3.35)$$

$$T_{em} = \frac{3}{2} p\left[\lambda_{PM} i_q + (L_d - L_q) i_d i_q\right] \qquad (3.36)$$

As v_q is the *q*-axis voltage, v_d is the *d*-axis voltage, i_q is the *q*-axis current, i_d is the *d*-axis current, *R* is the winding resistance of the stator, L_q is the *q*-axis inductance, L_d is the *d*-axis inductance, *p* is the of pole pairs number, *m* is the phases number, ω_e is the angular speed, λ_{PM} is the flux linkage of the permanent magnet and T_{em} is the electromagnetic torque (Caruso et al., 2017)

L_d, L_q, and PM are parameters that have constant values in the standard method. Numerous modeling strategies that consider saturation effects have been developed in the literature.

In more specific terms, the PM flux linkage and the dq-axes inductances are both functions of the dq-axes currents and the q-axis current, respectively. These IPMSM modeling techniques solely take into account the effects of the basic elements, ignoring the harmonic field components brought about by the interaction of saturation, cross-coupling, slotting, and permeance variance with rotor position (Caruso et al., 2017).

3.3. Experimental Work

3.3.1. Prototype preparation

Preparation of a manufacturing an electrical motor can involve assembling a variety of parts, which can include winding wire, armature, stator, and bearings which is necessary to ensure a consistent result. The motors must be carefully inspected throughout the entire process, in order to make sure that they are manufactured to specification. After assembly, testing is typically done to ensure the quality and performance of the motor.

Isolators:
An isolator must be used to prevent a short circuit from occurring in case the coil's copper wire touches the stator laminations. In this instance, an epoxy fiberglass isolation bands made by PUCARO Germany was used.

In the stator, 12 pieces with the dimension of 40 x 50 mm were cut and arranged in the following manner as in Figure 3.13:

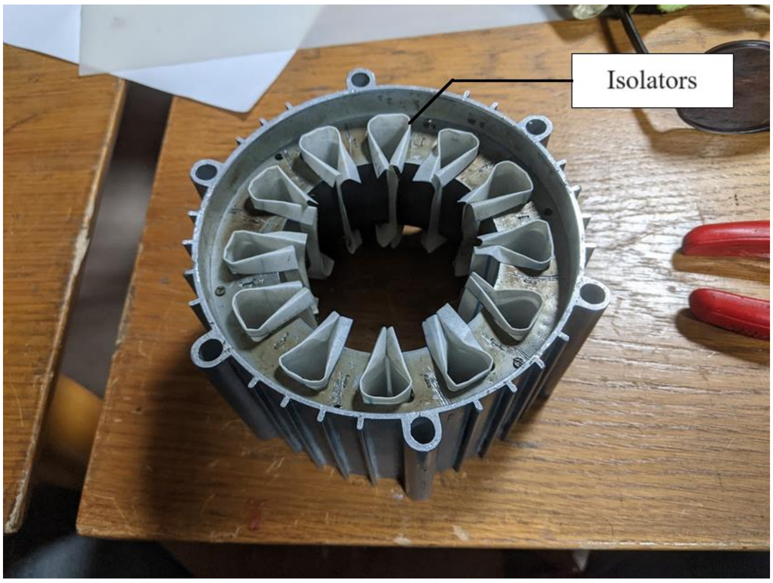

Figure 3.13 Isolators preparation

Winding scheme:
The winding process can begin after the isolation bands have been properly placed.

According to the Bavaria winding scheme calculator website (Niessen F., 2013) the winding scheme used was as in Figure 3.14: AabBCcaABbcC as started with phase A where the winding enters from tooth number 1 and carry on in the opposite direction to tooth number 2 then to tooth number 7 right to tooth number 8 in the opposite direction. The same process applied to phase B and C.

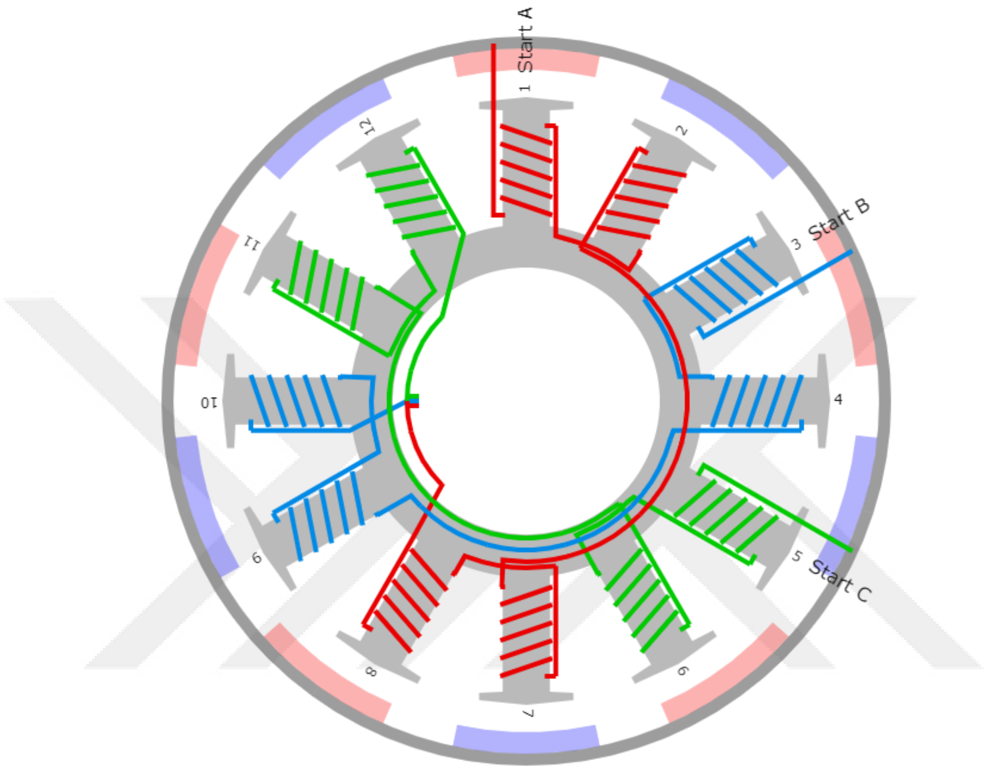

Figure 3.14 Winding scheme

To begin, 40 turns were wound on each yoke of phase A, followed by another 40 for phase B and the same for phase C as shown in Figures 3.15, 3.16 and 3.17.

Figure 3.15 Winding A phase

Figure 3.16 Winding A-B phases

Figure 3.17 Winding A-B-C phases

This procedure was repeated three times for each phase, until each slot had a total of 240 conductors.

This method of winding provides balanced resistance because the copper wire lengths are nearly equal for all three phases.

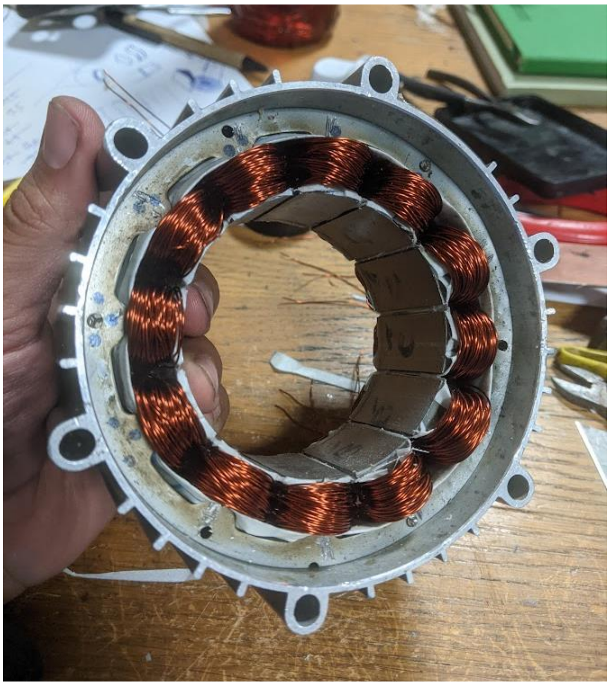

Figure 3.18 Fully winded

Wiring the cables:
After the winding process is complete, isolating the junction point between the copper conductor and the phase wires must be done, as well as the Y (Star) junction point. A fiberglass thermoresistant isolator was used for the wires joints to prevents contact and short circuit. To ensure that everything is correctly done, and for safety reasons, some measurements such as resistance and inductance checks, as well as phase body checks, must be performed.

After gathering all the parts together, a mechanical check is performed if there any friction between the rotor and the stator or any other mechanical problem.

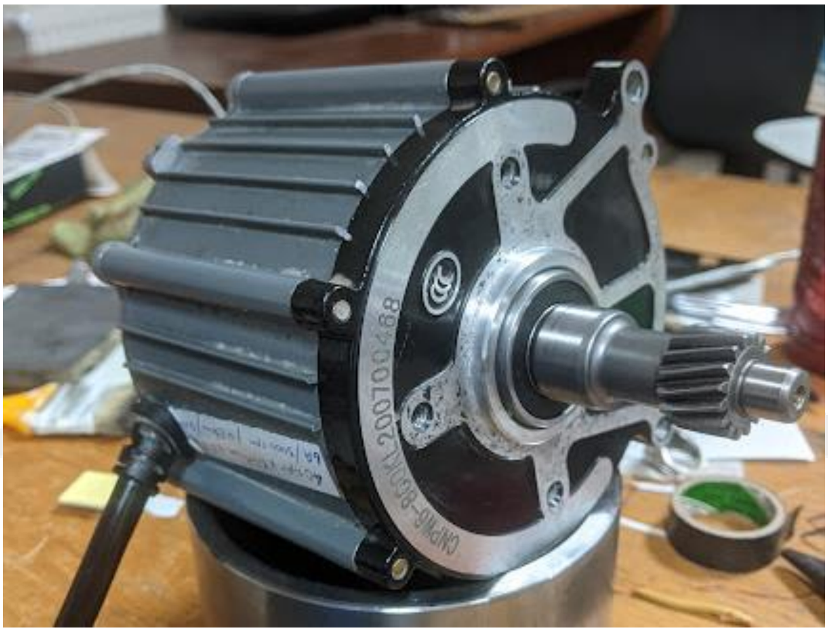

Figure 3.19 All the parts gathered together

Preparing the bench:
Due to the motor's dimensional incompatibility with the test bench, an external support (made of aluminum Sigma profile) was added to keep the test bench's axis aligned with the motor's axis as in figure 3.20. This external support is fixed to the deck of the test bench with thick brackets to prevent vibration and keep it snug and rigid.

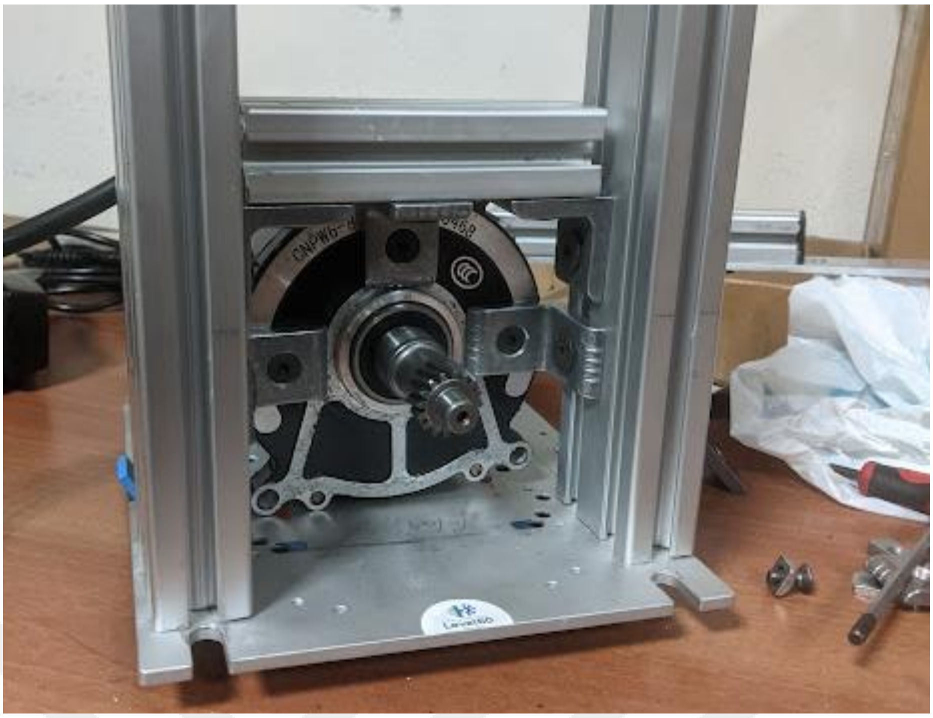

Figure 3.20 Fixed to the deck of the test bench

3.3.2. Driver's setup

The Control Unit CU310-2 PN (PROFINET) is a control module for single drives in which the open-loop and closed-loop control functions of the drive are implemented.

It controls the Power Modules in the block size format via the PM-IF interface and is mounted

directly on the Power Module as illustrated in figure 3.21 and 3.229. Power Modules Chassis are controlled from the Control Unit

via the DRIVE-CLiQ interface.

In this experimental work, Siemens Sinamics control unit CU310 DP and Siemens power module 340 were used to drive the motor using the provided software (Siemens STARTER).

Features of the driver:

- PROFIBUS as an external communication interface
- LAN (Ethernet)
- TTL/HTL/SSI - encoder evaluation
- Analog setpoint input

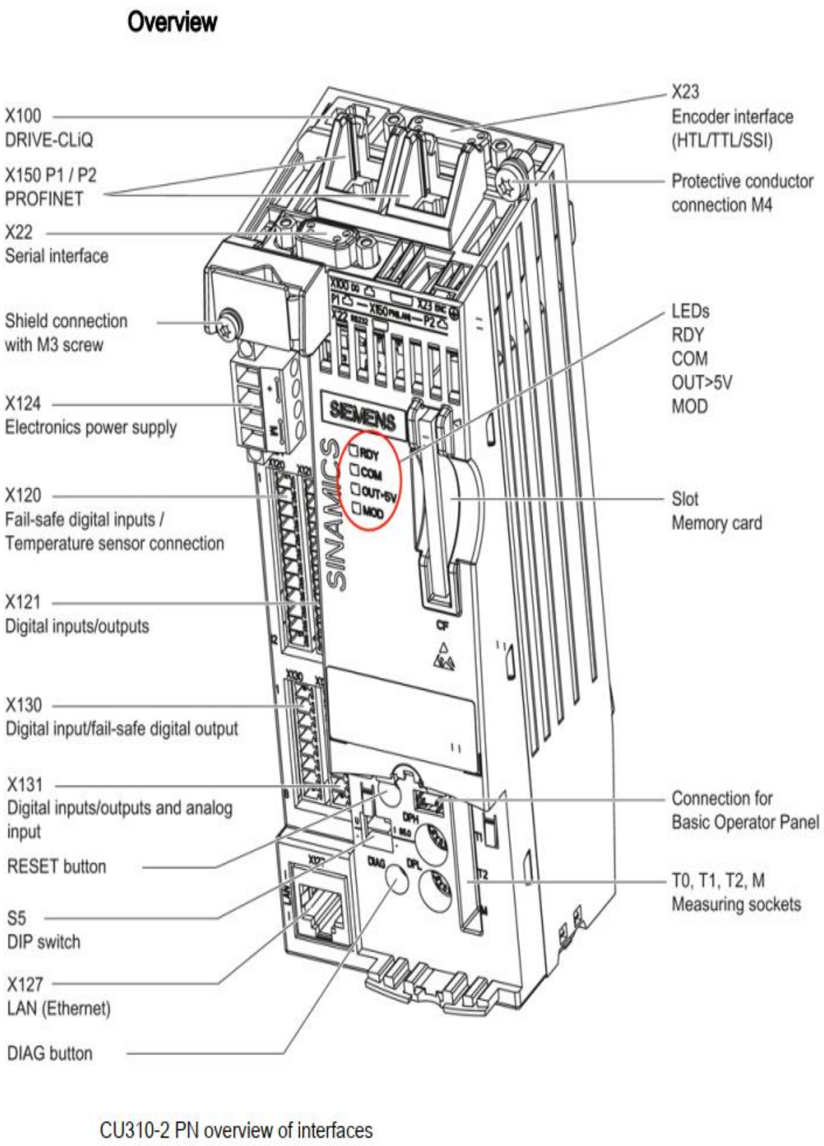

Figure 3.21 Sinamics control unit PM340

Technical features of the Power module: SINAMICS PM340:

Input voltage: 3AC 380-480V

Rated input current: 13.4 A

Resistance value: ≥ 75 Ω

Source frequency: 50/60Hz

Class of protection: IP20

Weight: 3.1 kg

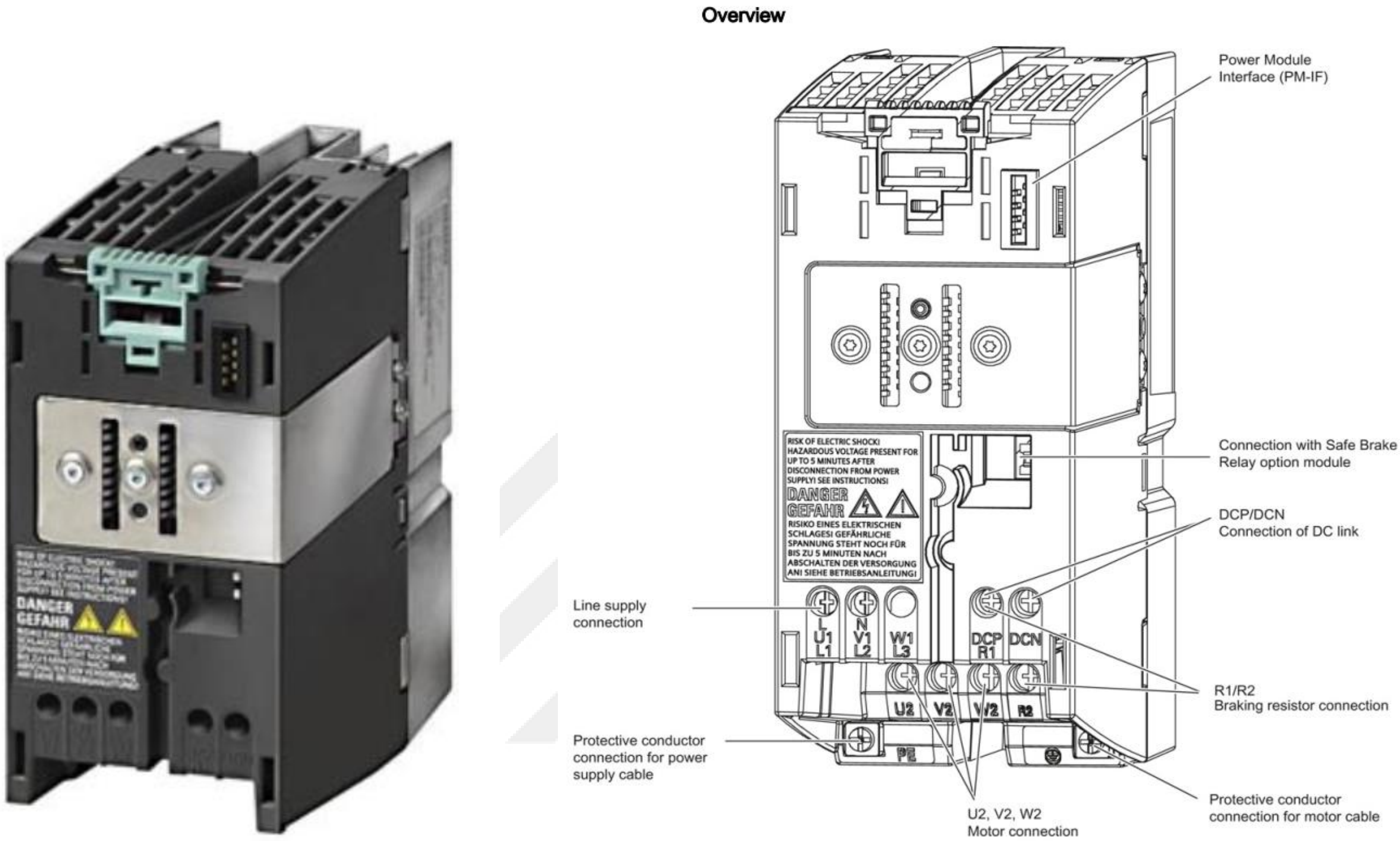

Figure 3.22 Sinamics power module

Requirements for commissioning:

The following are necessary for commissioning a SINAMICS S drive system:

● A programming device (PG/PC)

● STARTER commissioning tool

● A communication interface, e.g., PROFIBUS, PROFINET, Ethernet, CAN bus or USS (RS232-C)

● Completely wired-up drive line-up

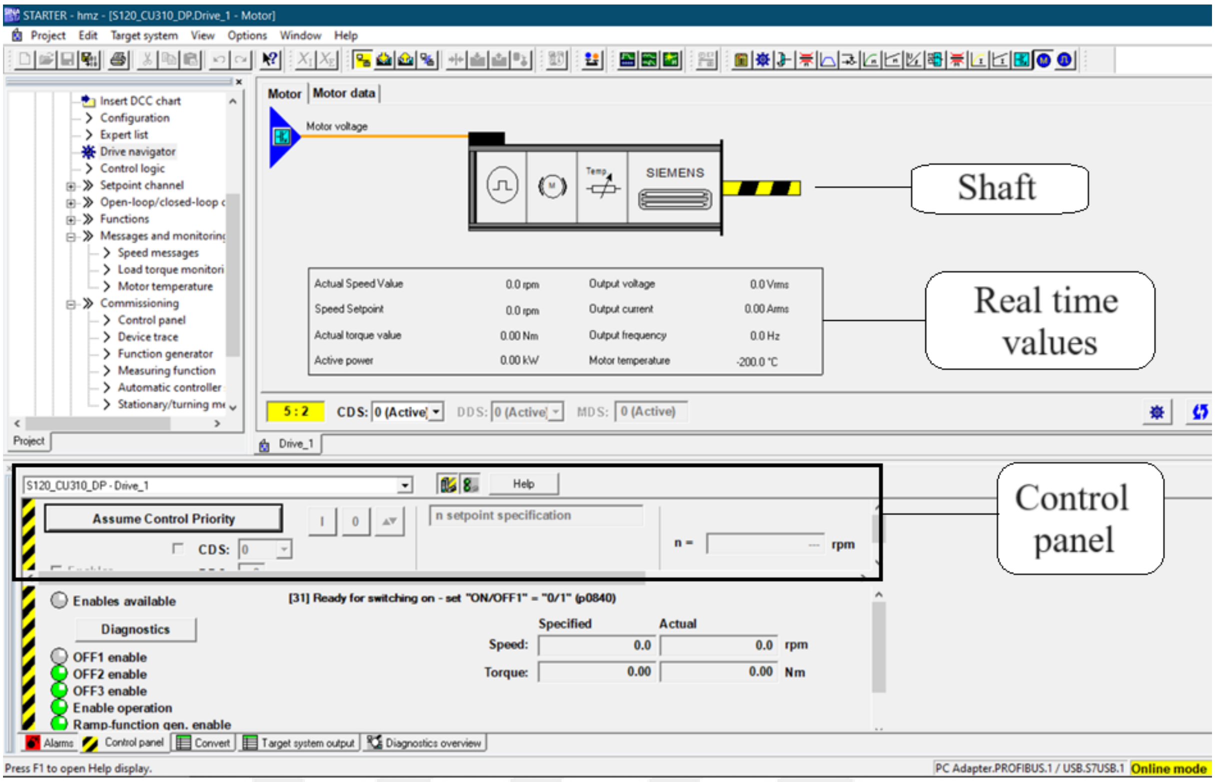

Figure 3.23 Siemens Starter user interface

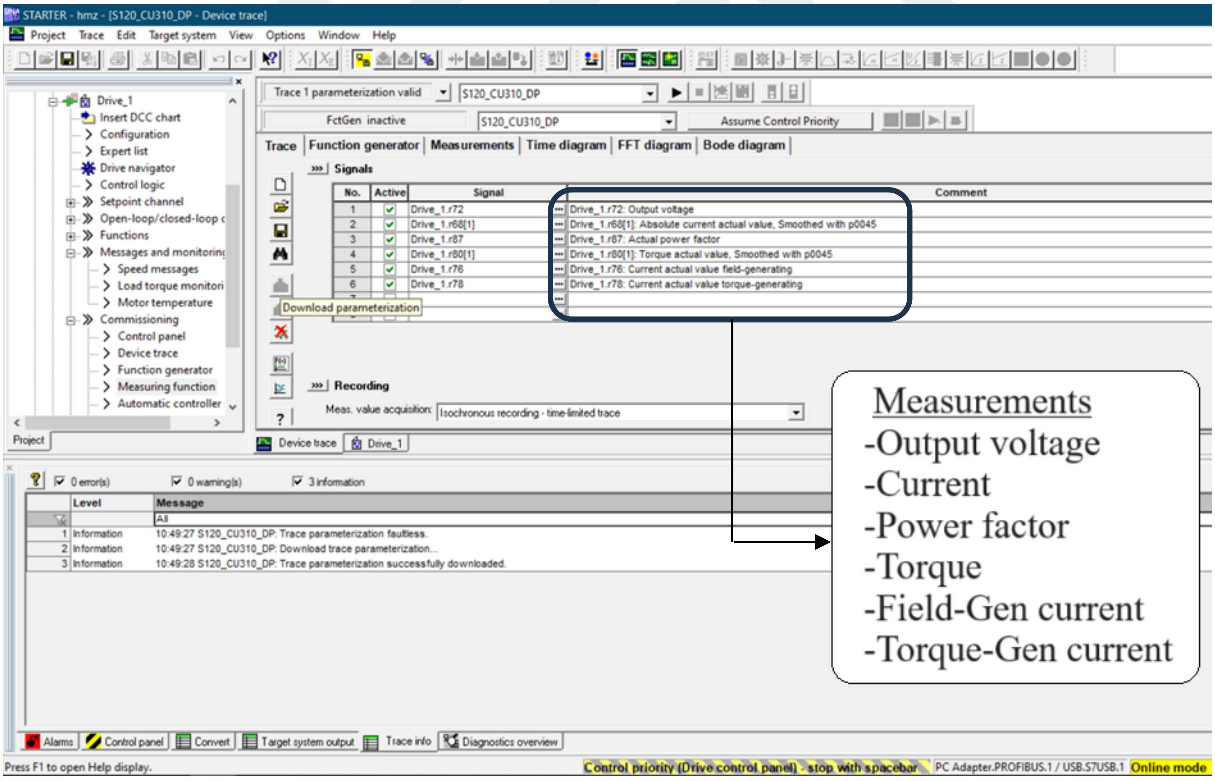

Figure 3.24 Siemens Starter measured parameters

After connecting the motor wires, power source, and USB link to the computer, the motor parameters should be properly defined according to its rated values. In this case,

Rated motor voltage: 200 V_{rms}

Rated motor current: 4.50 A_{rms}

Rated motor power: 1 KW

Rated motor speed: 3000 rpm

Rated motor frequency: 250 Hz

Motor identification: Standstill (doing a self-identification will be a good idea for the very first start).

The following settings of the motor driver had been configured as follow:

Control mode: Closed-loop as in Figure 3.23

Control type: Sensorless

Connection voltage: 380 – 480 / 3-Phase VAC

Cooling method: Internal air cooling

Power unit application: Load duty cycle with high over load for vector drives

Motor type: Synchronous motor (rotating, permanent magnet)

The (PMSM) can be elegantly controlled by using field-oriented theory to control space vectors of magnetic flux, current, and voltage. The PMSM can be made to perform exceptionally well dynamically by setting up the coordinate system to decompose the vectors into an electro-magnetic field generating part and a torque generating part. This results in a motor controller structure that is almost identical to that of a separately excited DC motor, making the PMSM easier to control as reflected in figure 3.25.

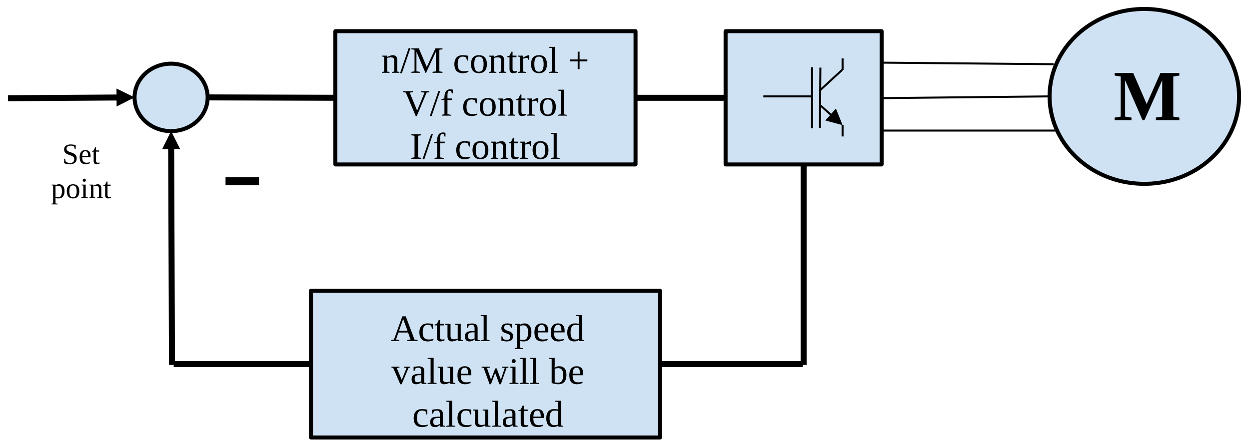

Figure 3.25 Motor control block diagram

3.3.3. Testing on the bench

To perform a proper test, the motor should be warmed up to 75°C before taking any measurements to ensure that the resistance value of the copper coils is correctly observed.

The braking torque was initially set from FESTO test bench at 0.5 Nm and then gradually increased by 0.5 Nm up to 4 Nm. The rotation speed was set from Siemens STARTER at 250 rpm and gradually increased by 250 up to 3000 rpm. In order to take the measurements, a braking system must be applied to the drive shaft of the motor, in this case, FESTO TP 1410 Servo brake and drive system was used.

The equipment set TP 1410 servo brake and actuator system, abbreviated motor test bench, is a complete load and actuator system. It allows the systems under examination to be analyzed in different load situations.

Simple tests can be performed also without a PC and software, such as recording a characteristic curve. The integrated display shows measured values, characteristics and the function mode.

Adapted to the servo brake and actuator system of Festo Didactic, the convenient software DriveLab provides a wide range of options.

The bench supports the following motor types:

• Single-phase and three-phase actuators

• DC actuators

• Modern servo drives.

Table 3.6 Festo Didactic servo brake system parameters

General information		
Dimension (H x W x D in mm)	510 x 380 x 270	mm
Weight	22	kg
Ambient conditions	5 – 40 relative humidity up to 65%	℃
Noise level	< 80	dB
Rotational speed setting range	+ 4000 to – 4000	rpm
Torque setting range	+ 4 to – 4	Nm
Braking power	Max 400, nominal 250	W
Supply voltage	AC 110 – 230	V
Input frequency	50 – 60	Hz
Input power	800	W

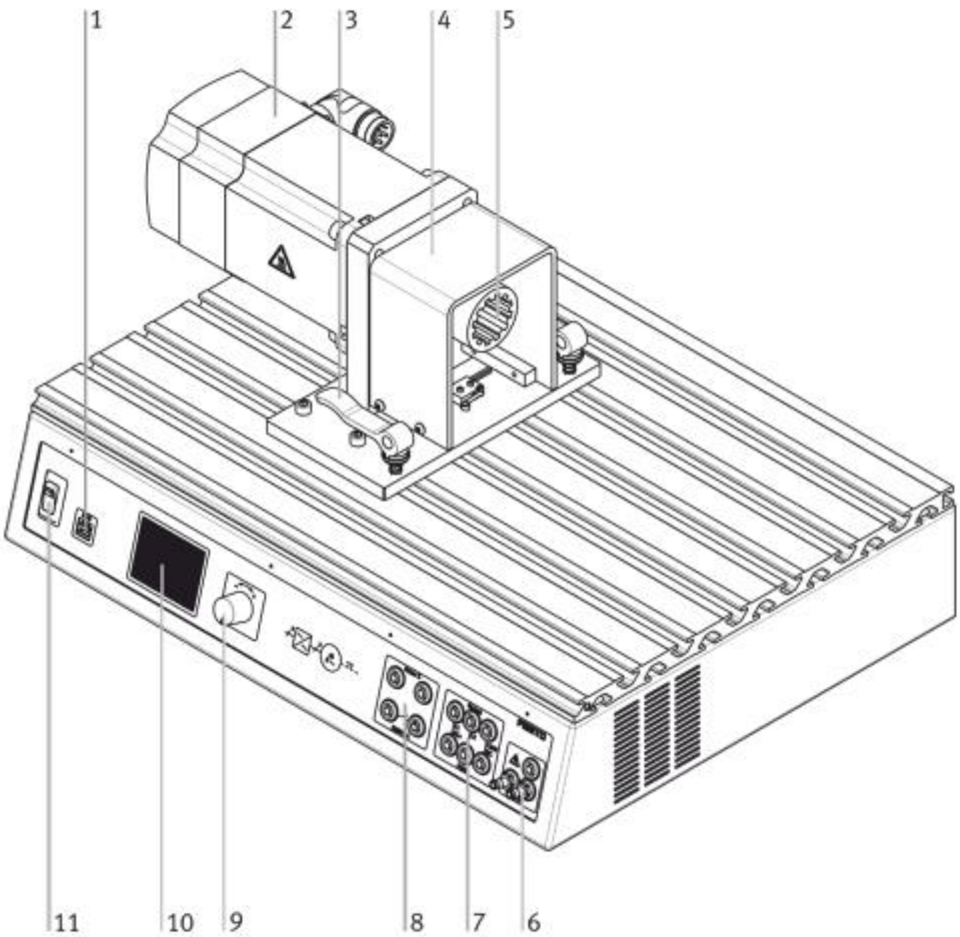

1: USB port
2: Servo brake motor
3: Quick clamping lever
4: Safety guard
5: Plug-in coupling
6: PE+ / protective grounding terminal
7: Test specimen connection field
8: Terminals for switching output (potential-free) and temperature switch input
9: Rotary knob
10: Display
11: Mains switch for server brake motor

Figure 3.26 Festo Didactic servo brake and actuator system description

Operating the bench (without PC):

The test bench is controlled by a rotary knob where the feedback can be observed on the display.

The bench can be operated in two ways:

- Torque Control = Setting the desired torque value by rotating the knob over the entire speed range.
- Speed Control = Setting the desired rotation speed by rotating the knob over the entire torque range.

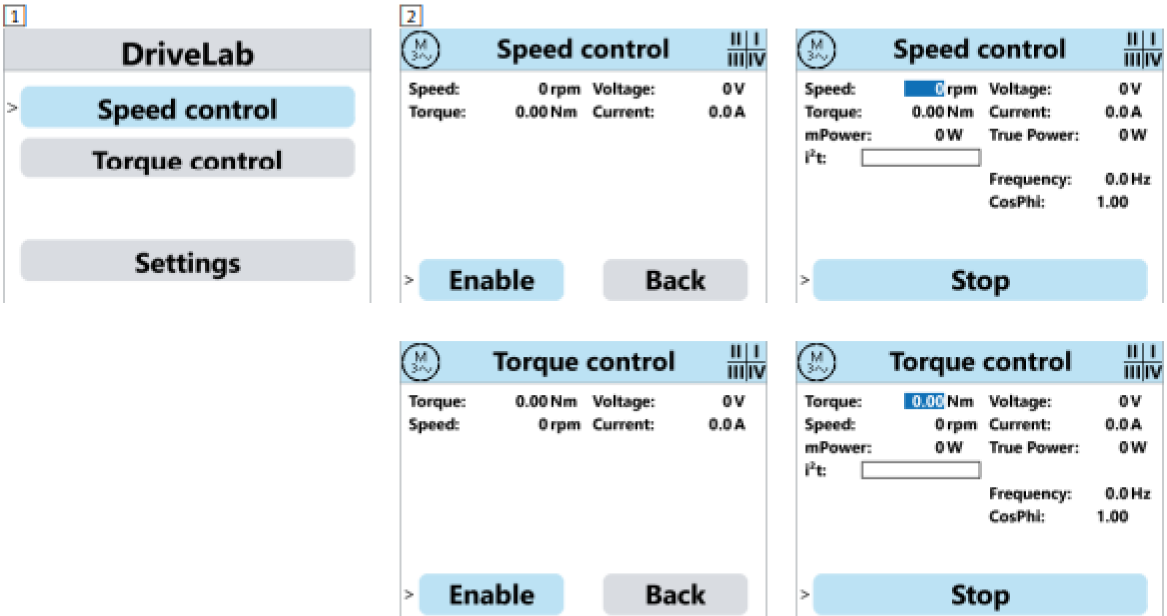

Figure 3.27 Festo Didactic servo brake and actuator built-in operation interface

4. RESULTS AND DISCUSSION

Taking measurements of an electrical motor is an important step in the motor's installation and maintenance. Measurements must be taken to ensure that the motor is receiving the proper power supply and running at the correct voltage, current, and frequency. Additionally, certain measurements can provide information about the motor's operating temperature, efficiency, vibration levels and bearing wear.

In the design process of an electric motor, thermal analysis results are very important for motors with magnets. Where the influence of overheating causes distortions in the structure of the magnets. The distortions cause losses in the fluxes produced by the magnets. As a result, magnetic flux densities decrease. If the amount of flux decreases below the amount required for the motor, it will lead to a decrease in motor efficiency and may not meet the requirements for the motor.

In this section, details of the experimental studies carried out to determine the performance characteristics of the prototyped IPMSM are provided. In the experimental studies, the speed, power and torque produced by the motor under different operating conditions and the current drawn by the motor were measured. The results obtained and the comparison of the results with the FEM analysis results are given in this section.

This type of motors can show higher performance in applications where the load varies proportional to the speed. For this reason, the studies have been extended to include fan type speed dependent loads as well as motor constant loads. The performance of the prototype under different constant load values is analyzed in this section. The obtained experimental and FEM analysis results are compared with each other.

The figures below show the efficiency map for both simulation and experimental work.

The maximum efficiencies of electric machines throughout a range of torque-speed operating points are displayed on efficiency maps providing an overview of the methods that can be used to calculate efficiency maps and provides a general grasp of traction motor modeling and interpretation. It displays the trade-off between accuracy and calculation effort for various techniques. An explanation is given of the efficiency map calculating procedure for permanent magnet synchronous machines and sample induction motors as the figures 4.1 and 4.2 below show the efficiency map for both simulation and experimental work.

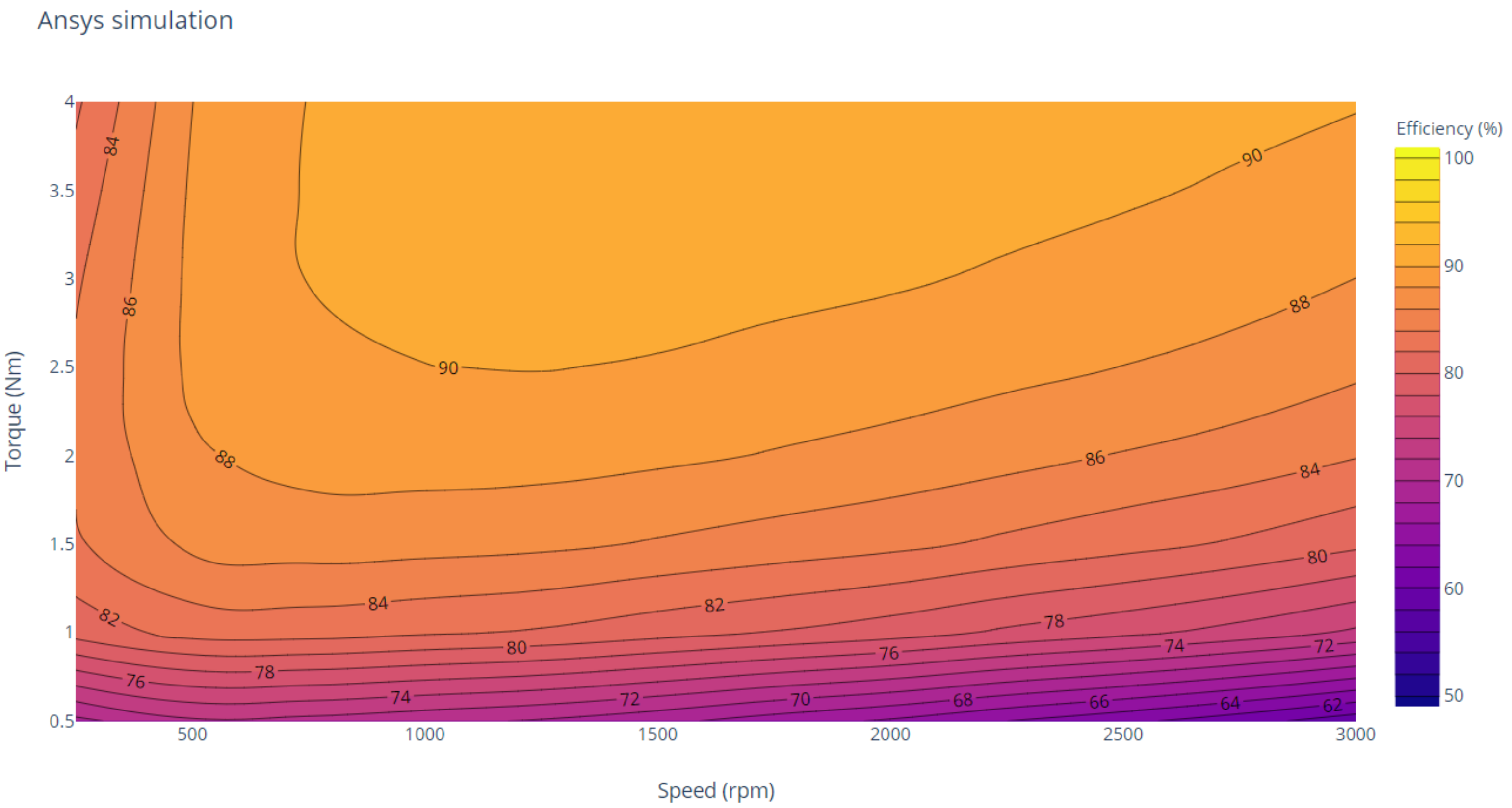

Figure 4.1 Simulation analysis efficiency map

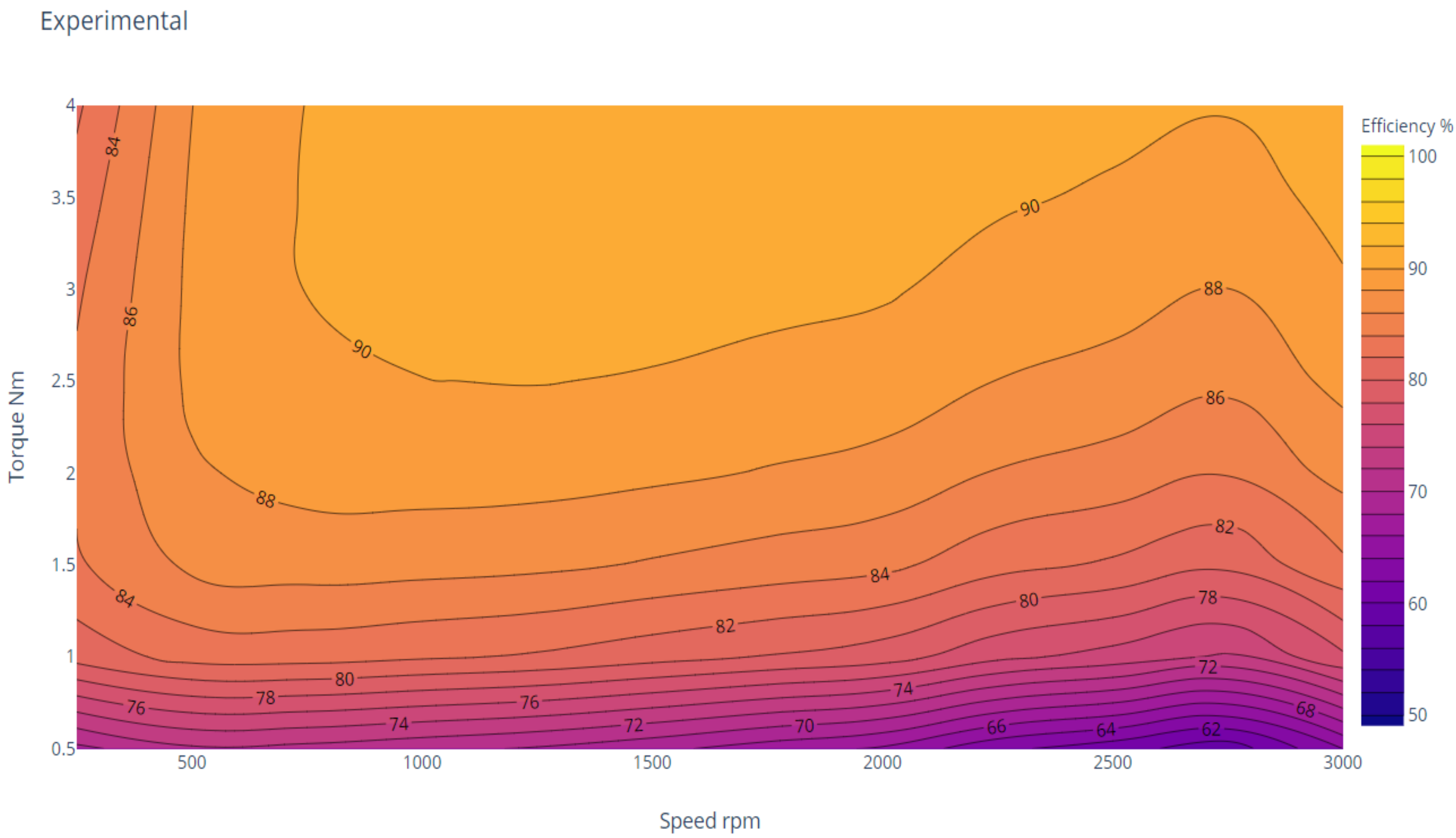

Figure 4.2 Experimental analysis efficiency map

In the experiments conducted, the transient performance of the motor under different constant loads was analyzed. In this context, the motor is first tested separately for each fixed load with an operation range from 0.5 Nm to 4.5 Nm. During the test period, power, current, cos φ, efficiency, torque, etc. parameters of the motor have been recorded. According to the data obtained, the variation of efficiency and power factor depending on the output power is analyzed. A general evaluation of the findings obtained as a result of the design and optimization studies was made. As can be seen from the graph, 2D FEM analysis was used in the performance evaluation of the model in order to shorten the analytical analysis time.

In this section, all dimensioning and optimization has been done using the ANSYS Electronics Software where the efficiency and other output parameters are kept at the desired values then parametric solutions were applied and the motor model was obtained.

Figure 4.1 shows the graphs of the efficiency values obtained in the simulation depending on the motor speed and torque values. The highest efficiency values were obtained at 3000 rpm. On the other hand, as shown in Figure 4.2 the maximum value for the efficiency was at 2750 rpm however, it is noticed that the efficiency value decreases after 2750 rpm.

Figure 4.3 shows the graph of average torque depending on the variation of the speed. As can be seen from the graph, the torque value is almost constant according to the speed. However, it is seen that at the speed of 2790 rpm the torque values start to decrease.

The graphs of important parameters generated with RMxprt are given below in Figure 4.5, where the graph of the change in current obtained depending on the speed is given. It is clearly observed that the change in motor current decreases as the motor speed increases.

The analysis of the electric motor revealed results that showed its speed, torque, voltage, and current. The figures below reflect the achieved performance of the motor, with a maximum speed of 3425 rpm and a torque of 4.88Nm. The voltage applied to the motor was 173.52 V, with a maximum current of 5.39 A. This result clearly indicates that this motor is an efficient and reliable choice for most applications. Furthermore, these figures demonstrate that the motor has a good response to various inputs and that its overall performance can be trusted.

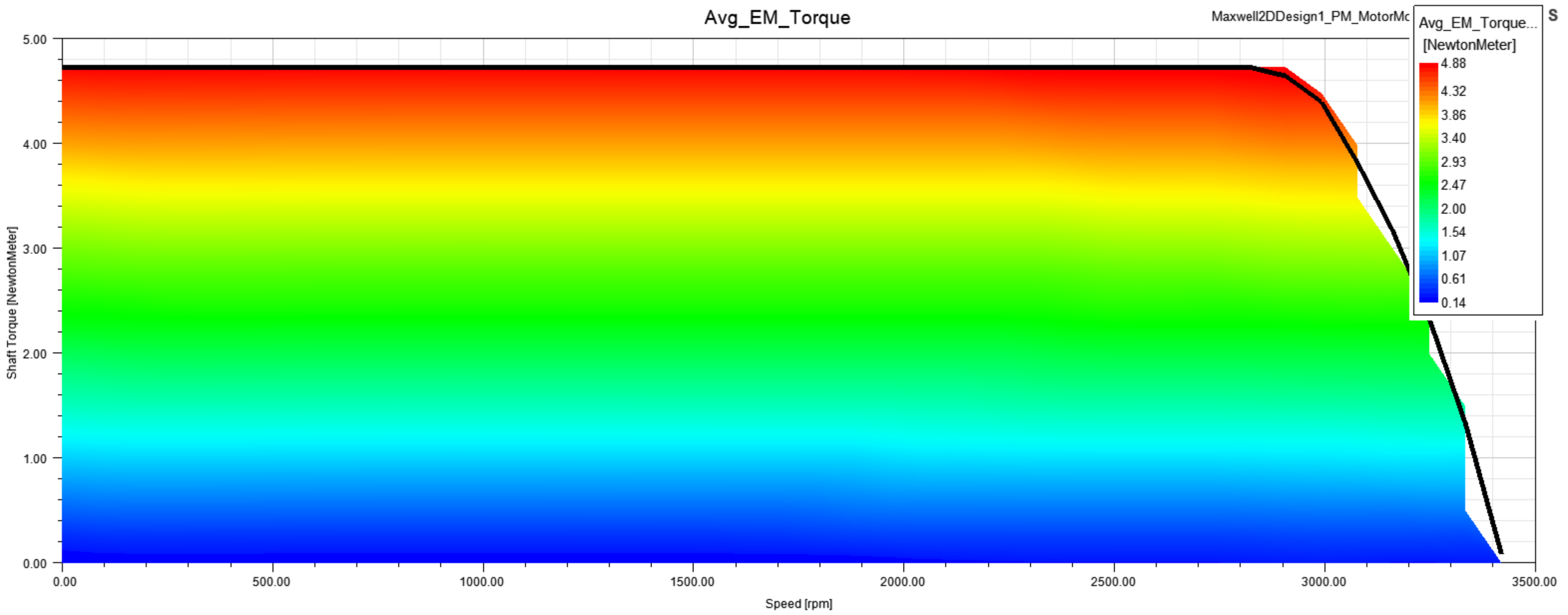

Figure 4.3 Average torque

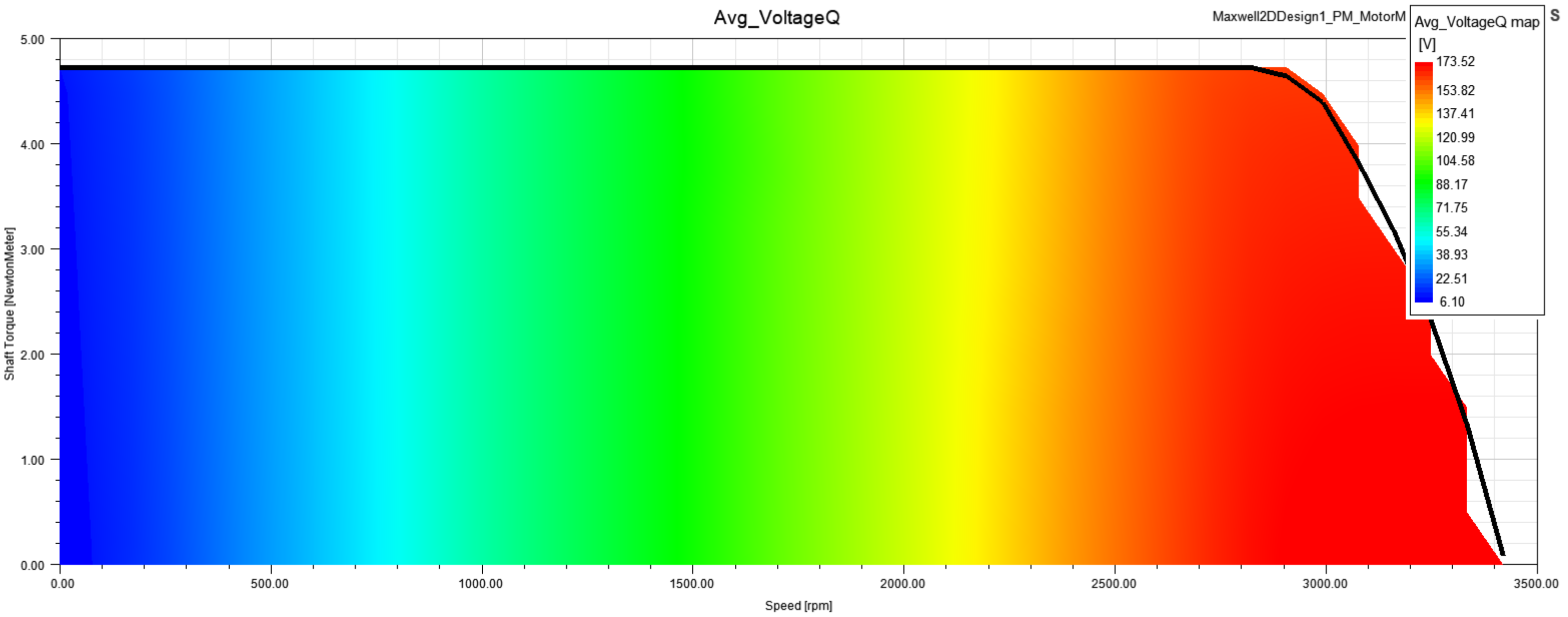

Figure 4.4 Average voltage

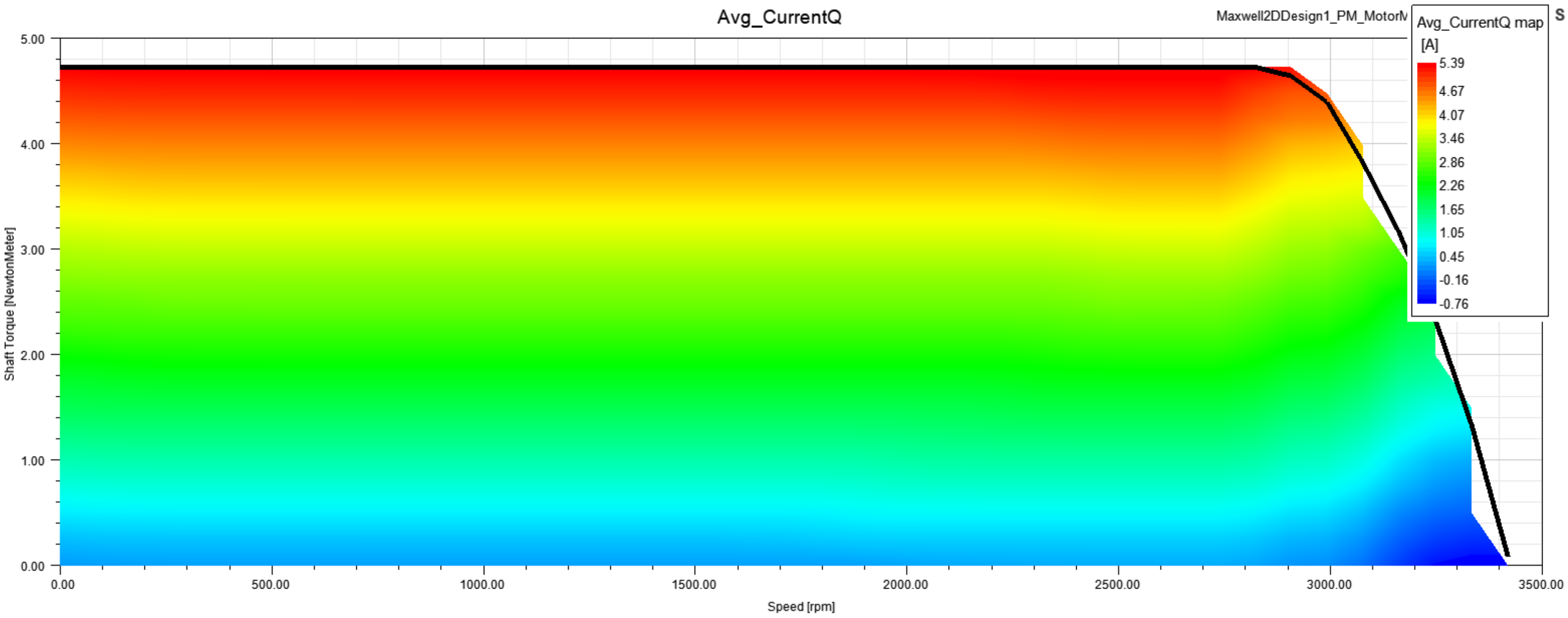

Figure 4.5 Average current

Table 4.1 comparison of the simulation and experimental results

Design parameters	Simulation	Experimental	Error
Efficiency	91%	89%	2%
Speed	3082 rpm	3000 rpm	82 rpm
Rated torque	3.39 Nm	4.0 Nm	0.61 Nm

As a result, the experimental study of the electric motor was nearly close to the simulation. Both the experimental and the simulated process produced reliable results. The results of the experiment and the simulation can be seen in the appendix section below (Table 7.1 and Table 7.2). The experiment showed that the motor torque at 4.0 Nm with an input voltage of 212 V and a speed of 3000 rpm reached the efficiency of 89 %, where in simulation, the results indicated that the motor torque at 4.0 Nm and at the speed of 3000 rpm with an input voltage of 163.9 V reached the efficiency of 90.13 %. The results of the experiment and the simulation demonstrate that the motor is performing almost as expected. The slight variation between the experimental and the simulated results can be attributed to small differences in the environment, such as power supply voltage, temperature, and other external factors. In conclusion, the experimental and simulation comparison of the electric motor successfully produced accurate and reliable results. The results demonstrate that the motor is functioning properly and that the simulation closely matched the experimental data.

5. CONCLUSION AND RECOMMENDATION

The design of the 220 V, 3000 rpm IPMS motor began with a meticulous analysis of its physical, magnetic, and thermal requirements. This involved extensive literature review and a thorough examination of academic studies to gather relevant information and established design methodologies. Utilizing this knowledge, the required input parameters for the motor design were meticulously determined. Complex calculations were undertaken, incorporating specific motor properties and established design equations. This process formed the foundation for the entire design process.

At the design stage, careful attention was paid to the properties of the motor's components and the selection of optimal materials. Factors such as ease of implementation, functionality, and material properties were meticulously considered. The stator, rotor, and sheet metal used in the motor were subjected to comprehensive analyses, encompassing both their magnetic and thermal performance. Additionally, the magnetic values of the magnets and other materials were thoroughly evaluated. This meticulous analysis proved crucial in achieving a robust and efficient motor design.

The results of the comprehensive material and design analyses were combined with the previously determined input parameters to form a comprehensive understanding of the motor's intended characteristics. By drawing necessary inferences from this information, the initial design of the motor was developed. This iterative process helps to refine and optimize the design, ensuring optimal performance and achieving the desired torque, power, and speed values.

The culmination of the design process involved the utilization of Ansys Maxwell RMxprt software. This tool used to meticulously refine the initial design and assess its performance. The motor's dimensions, number of slots and poles, winding model, and various constant and variable parameters were meticulously transferred into the software, allowing for a comprehensive simulation of the motor's operation.

The Ansys Maxwell RMxprt software provided invaluable insights into the motor's performance characteristics. A crucial aspect of the design process involved analyzing the material saturation points within the motor. This analysis ensured that the chosen materials would operate within acceptable limits, preventing potential performance degradation or motor failure. By carefully analyzing the saturation points and iteratively refining the design, the motor's efficiency optimized and minimized the potential risks.

Based on the numerous advantages demonstrated throughout this project, the extensive use of IPM motors across diverse industries is strongly recommended. These motors offer a compelling combination of improved torque characteristics, higher efficiency over a wide range of speeds, and superior reliability and robustness compared to traditional motor designs.

Such benefits make them ideal candidates for numerous applications, including:

Industrial: Robotics, machine tools, pumps, and other industrial automation equipment.

Domestic: Appliances, power tools, electric vehicles, and other home appliances.

Emerging: Renewable energy systems, aerospace, medical devices, and other innovative applications.

While IPM motors offer significant advantages, further research and development are crucial to maximize their potential. This includes focusing on:

Cost reduction: Exploring new manufacturing processes and advanced materials to make IPM motors more affordable.

Performance improvement: Optimizing motor design for specific applications and developing innovative control strategies to further enhance performance.

Smart technology integration: Integrating smart sensors and monitoring systems into IPM motors for real-time performance analysis and diagnostics.

By continued research and development across these key areas, IPM motors will continue to evolve and become even more efficient, cost-effective, and versatile. This will undoubtedly lead to their widespread adoption and revolutionize the way we utilize electric motors in a multitude of applications.

6. REFERENCES

Agamloh, E., von Jouanne, A., & Yokochi, A. (2020). An Overview of Electric Machine Trends in Modern Electric Vehicles. *Machines*, *8*(2), 20. https://doi.org/10.3390/machines8020020

Akatsu, K., Narita, K., Sakashita, Y., & Yamada, T. (2008). Characteristics comparison between SPMSM and IPMSM under high flux density condition by both experimental and analysis results. *2008 International Conference on Electrical Machines and Systems*, 2848–2853.

Akgün G. (2013). *2x400 Tone Portal Crane Design and Numerical Analysis* [Master's Thesis] İstanbul Teknik University, İstanbul.

Alger, P. L., & Arnold, R. E. (1976). The history of induction motors in America. *Proceedings of the IEEE*, *64*(9), 1380–1383. https://doi.org/10.1109/PROC.1976.10329

An, H.-J., Lee, S.-K., Kang, G.-H., & Kim, B.-W. (2016). Rotor design optimization for performance improvement of IPM motor. *2016 IEEE Conference on Electromagnetic Field Computation (CEFC)*, 1. https://doi.org/10.1109/CEFC.2016.7816267

Bojoi, R., Armando, E., Di Torino, P., Energia, D., Brüel, H.-H., & Kjaer, &. (n.d.) (2023). *Efficiency And Loss Mapping Identification Procedure*. from https://www.hbm.com/en/6207/white-paper-efficiency-and-loss-mapping-of-ac-motors/ 02/06/2023.

Caruso, M., Di Tommaso, A. O., Miceli, R., Nevoloso, C., Spataro, C., & Viola, F. (2017). Enhanced loss model algorithm for interior permanent magnet synchronous machines. *2017 AEIT International Annual Conference*, 1–6. https://doi.org/10.23919/AEIT.2017.8240580

Choi, Y., Kim, N.-H., Jung, S.-W., & Jung, S.-Y. (2022). Robust Design Method for Surface-Mounted Permanent Magnet Motor with Two-slot Pitches Winding Considering Eccentricity. *2022 IEEE 20th Biennial Conference on Electromagnetic Field Computation (CEFC)*, 1–2. https://doi.org/10.1109/CEFC55061.2022.9940802

Dönmezer, Y., (2009). *Reduction of Torque Vibrations in Brushless Direct Current Motors* [Master's Thesis]. İstanbul University, Informatics Institute.

Ge, X., (2014). *Simulation Of Vibrations İn Electrical Machines For Hybrid-Electric Vehicles* [Master's Thesis]. Chalmers University of Technology Göteborg, Sweden.

Gudivada, R., Bodnapu, K. K., & Vavillapalli, K. R. (2017). Virtual characterization of Interior Permanent Magnet (IPM) motor for EV traction applications. *2017 IEEE Transportation Electrification Conference (ITEC-India)*, 1–4. https://doi.org/10.1109/ITEC-India.2017.8333875

Helwig, A. (1995). History and development of non-intrusive electrical testing and assessment of DC traction motor armature condition and reliability during overhaul. *1995 Seventh International Conference on Electrical Machines and Drives (Conf. Publ. No. 412)*, 111–115. https://doi.org/10.1049/cp:19950845

K. Chari, M. (1974). Finite-Element Solution of the Eddy-Current Problem in Magnetic Structures. *IEEE Transactions on Power Apparatus and Systems*, *PAS-93*(1), 62–72. https://doi.org/10.1109/TPAS.1974.293916

Li, B., & Wang, C. (2016). Comparative analysis on PMSM control system based on SPWM and SVPWM. *2016 Chinese Control and Decision Conference (CCDC)*, 5071–5075. https://doi.org/10.1109/CCDC.2016.7531902

Michalowicz, J. C. (1948). Origin of the electric motor. *Electrical Engineering*, *67*(11), 1035–1040. https://doi.org/10.1109/EE.1948.6444428

Mohanraj, D., Aruldavid, R., Verma, R., Sathiyasekar, K., Barnawi, A. B., Chokkalingam, B., & Mihet-Popa, L. (2022). A Review of BLDC Motor: State of Art, Advanced Control Techniques, and Applications. *IEEE Access*, *10*, 54833–54869. https://doi.org/10.1109/ACCESS.2022.3175011

Niessen F., (2013). *Winding Scheme Calculator*. Skylar. https://www.bavaria-direct.co.za/scheme/calculator/ 28/10/2023

Niu, C., & Chen, T. (2022). Analysis of the Influence of the Shape and Distribution of Permanent Magnets on the Torque Ripple of Surface Mounted Permanent Magnet Motors. *2022 2nd International Conference on Consumer Electronics and Computer Engineering (ICCECE)*, 694–697. https://doi.org/10.1109/ICCECE54139.2022.9712769

Okur, M. (2007). *Design and Construction of a Four Stroke, Single Cylinder, Spark Ignition Gasoline Engine Using Finite Element Method* [PhD Thesis]., Gazi Universitesi, Ankara.Pyrhnen, J. , J. T. ve H. V. , 2008. (2008). *Design of Rotating Electrical Machines*. John Wiley and Sons, 584 p, Chichester UK.

Rahman, M. A., Masrur, M. A., & Uddin, M. N. (2012). Impacts of interior permanent magnet machine technology for electric vehicles. *2012 IEEE International Electric Vehicle Conference*, 1–5. https://doi.org/10.1109/IEVC.2012.6183226

Rahman, Md. A. (2013). History of interior permanent magnet motors [History]. *IEEE Industry Applications Magazine*, *19*(1), 10–15. https://doi.org/10.1109/MIAS.2012.2221996

Sahin, F., 2001. (2001). *Design and development of a High-speed axial-flux permanent Machine* [Ph. D. Thesis]. Technische Universiteit Eindhoven.

Sakunthala, S., Kiranmayi, R., & Mandadi, P. N. (2017). A study on industrial motor drives: Comparison and applications of PMSM and BLDC motor drives. *2017 International Conference on Energy, Communication, Data Analytics and Soft Computing (ICECDS)*, 537–540. https://doi.org/10.1109/ICECDS.2017.8390224

Sebastian, T., Slemon, G., & Rahman, M. (1986). Modelling of permanent magnet synchronous motors. *IEEE Transactions on Magnetics*, *22*(5), 1069–1071. https://doi.org/10.1109/TMAG.1986.1064466

Takano, Y., Chiba, A., Ogasawara, S., Takeno, M., Hoshi, N., Imakawa, T., & Takemoto, M. (2010). Torque density and efficiency improvements of a Switched Reluctance Motor without rare earth material for hybrid vehicles. *2010 IEEE Energy Conversion Congress and Exposition*, 2653–2659. https://doi.org/10.1109/ECCE.2010.5618025

Tinazzi, F., Bolognani, S., Calligaro, S., Kumar, P., Petrella, R., & Zigliotto, M. (2019). Classification and review of MTPA algorithms for synchronous reluctance and interior permanent magnet motor drives. *2019 21st European Conference on Power Electronics and Applications (EPE '19 ECCE Europe)*, P.1-P.10. https://doi.org/10.23919/EPE.2019.8915144

Turhan, E., (2014). *Moment Improvement in External Rotor Brushless Direct Current Motors* [Master's Thesis]. Istanbul Technical University Institute of Science and Technology.

Ustun, O., & Kara, D. B. (2018a). Evaluation of Spoke Type IPM Synchronous Motors for IE4 Efficiency Class. *2018 XIII International Conference on Electrical Machines (ICEM)*, 1176–1181. https://doi.org/10.1109/ICELMACH.2018.8506864

Wang, X., Zhang, Z., Gao, P., Lu, H., & He, X. (2018). Design and Simulation Analysis of a Novel Outer Rotor IPM Motor Used in Electric Vehicles. *2018 13th World Congress on Intelligent Control and Automation (WCICA)*, 1413–1418. https://doi.org/10.1109/WCICA.2018.8630708

Yildirim, M., Polat, M., & Kürüm, H. (2014). A survey on comparison of electric motor types and drives used for electric vehicles. *2014 16th International Power Electronics and Motion Control Conference and Exposition*, 218–223. https://doi.org/10.1109/EPEPEMC.2014.6980715

Yoon, K.-Y., & Baek, S.-W. (2020). Performance Improvement of Concentrated-Flux Type IPM PMSM Motor with Flared-Shape Magnet Arrangement. *Applied Sciences*, *10*, 6061. https://doi.org/10.3390/app10176061

Zhang, D., Zhao, H., & Wu, T. (2017). The rotor copper and iron loss analysis of inverter-fed induction motor considering rotor slip frequency. *2017 IEEE Energy Conversion Congress and Exposition (ECCE)*, 2412–2419. https://doi.org/10.1109/ECCE.2017.8096465

Zhang, X., & Qu, R. (2013). Pole number selection strategy of low-speed multiple-pole permanent magnet synchronous machines. *2013 International Electric Machines & Drives Conference*, 1267–1274. https://doi.org/10.1109/IEMDC.2013.6556297

Zöhra, B., & Akar, M. (2021). Performance verification of novel rotor line start PMSM. *Journal of Mechatronics and Artificial Intelligence in Engineering*, *2*(2), 86–95. https://doi.org/10.21595/jmai.2021.22219

7. APPENDIX

Table 7.1 Experimental analysis values

Experimental results							
Speed	**Efficiency**	**Current**	**Power factor**	**Input power**	**Output power**	**Output Voltage**	**Torque**
rpm	**%**	A	Cos φ	W	**W**	V	Nm
250	62	1.60	0.406	20.94	13.08	18.61	0.50
250	79	1.17	0.984	33.13	26.17	16.61	1.00
250	81	1.60	0.983	48.63	39.25	17.84	1.50
250	82	2.02	0.971	63.94	52.33	18.82	2.00
250	83	2.28	0.974	78.98	65.42	20.53	2.50
250	81	2.83	0.957	96.64	78.50	20.60	3.00
250	81	3.00	0.963	112.88	91.58	22.55	3.50
250	80	3.29	0.960	130.20	104.67	23.80	4.00
Speed	**Efficiency**	**Current**	**Power factor**	**Input power**	**Output power**	**Output Voltage**	**Torque**
rpm	**%**	A	Cos φ	W	W	V	Nm
500	70	0.72	0.997	37.37	26.17	30.05	0.50
500	81	1.20	0.991	64.71	52.33	31.41	1.00
500	85	1.63	0.978	92.26	78.50	33.40	1.50
500	86	2.09	0.959	121.27	104.67	34.93	2.00
500	87	2.49	0.951	150.61	130.83	36.75	2.50
500	87	2.85	0.938	180.18	157.00	38.91	3.00

500	87	3.25	0.922	210.71	183.17	40.60	3.50
500	86	3.45	0.960	242.08	209.33	42.20	4.00

Speed	**Efficiency**	**Current**	**Power factor**	**Input power**	**Output power**	**Output Voltage**	**Torque**
rpm	**%**	A	Cos φ	W	W	V	Nm
750	70	0.73	0.986	55.71	39.25	44.67	0.50
750	81	1.24	0.985	96.92	78.50	45.83	1.00
750	85	1.73	0.978	138.36	117.75	47.23	1.50
750	87	2.20	0.966	181.42	157.00	49.30	2.00
750	88	2.68	0.957	224.00	196.25	50.44	2.50
750	89	3.10	0.946	264.35	235.50	52.03	3.00
750	89	3.55	0.935	310.40	274.75	54.00	3.50
750	89	3.90	0.940	354.31	314.00	55.80	4.00

Speed	**Efficiency**	**Current**	**Power factor**	**Input power**	**Output power**	**Output Voltage**	**Torque**
rpm	**%**	A	Cos φ	W	W	V	Nm
1000	69	0.71	0.988	76.19	52.33	62.71	0.50
1000	81	1.18	0.992	129.94	104.67	64.06	1.00
1000	85	1.66	0.980	184.73	157.00	65.53	1.50
1000	87	2.07	0.975	240.26	209.33	68.76	2.00
1000	88	2.55	0.949	297.61	261.67	71.03	2.50
1000	89	3.02	0.946	351.77	314.00	71.05	3.00

1000	89	3.50	0.932	409.50	366.33	72.51	3.50
1000	89	3.90	0.950	468.46	418.67	73.00	4.00

Speed	Efficiency	Current	Power factor	Input power	Output power	Output Voltage	Torque
rpm	**%**	A	Cos φ	W	W	V	Nm
1250	68	0.72	0.995	96.80	65.42	78.01	0.50
1250	80	1.20	0.995	164.05	130.83	79.31	1.00
1250	85	1.67	0.986	231.45	196.25	81.19	1.50
1250	87	2.15	0.963	299.72	261.67	83.60	2.00
1250	89	2.58	0.950	367.93	327.08	86.66	2.50
1250	89	3.00	0.958	439.19	392.50	88.25	3.00
1250	89	3.48	0.945	515.68	457.92	90.52	3.50
1250	89	3.87	0.950	587.12	523.33	92.20	4.00

Speed	Efficiency	Current	Power factor	Input power	Output power	Output Voltage	Torque
rpm	**%**	A	Cos φ	W	W	V	Nm
1500	67	0.73	0.994	116.64	78.50	92.84	0.50
1500	79	1.25	0.972	198.86	157.00	94.51	1.00
1500	84	1.74	0.964	281.37	235.50	96.82	1.50
1500	87	2.20	0.975	362.12	314.00	97.51	2.00
1500	88	2.67	0.945	446.33	392.50	102.17	2.50
1500	88	3.12	0.941	533.48	471.00	104.95	3.00

1500	89	3.58	0.947	614.59	549.50	104.66	3.50
1500	89	4.10	0.950	708.37	628.00	105.00	4.00

Speed	Efficiency	Current	Power factor	Input power	Output power	Output Voltage	Torque
rpm	%	A	Cos φ	W	W	V	Nm
1750	65	0.77	0.986	140.74	91.58	106.98	0.50
1750	78	1.27	0.985	235.70	183.17	108.81	1.00
1750	84	1.73	0.974	326.32	274.75	111.83	1.50
1750	86	2.23	0.968	427.18	366.33	114.24	2.00
1750	88	2.68	0.957	520.85	457.92	117.27	2.50
1750	89	3.17	0.948	620.67	549.50	119.21	3.00
1750	89	3.65	0.933	723.90	641.08	122.77	3.50
1750	89	4.05	0.940	824.24	732.67	125.00	4.00

Speed	Efficiency	Current	Power factor	Input power	Output power	Output Voltage	Torque
rpm	%	A	Cos φ	W	W	V	Nm
2000	64	0.79	0.981	164.01	104.67	122.14	0.50
2000	77	1.29	0.982	272.21	209.33	124.03	1.00
2000	83	1.77	0.971	379.70	314.00	127.57	1.50
2000	86	2.23	0.962	486.90	418.67	131.06	2.00
2000	88	2.68	0.954	592.81	523.33	133.86	2.50
2000	89	3.18	0.942	709.49	628.00	136.75	3.00

2000	89	3.67	0.926	826.71	732.67	140.44	3.50
2000	90	4.01	0.935	931.90	837.33	143.50	4.00

Speed	**Efficiency**	**Current**	**Power factor**	**Input power**	**Output power**	**Output Voltage**	**Torque**
rpm	**%**	A	Cos φ	W	W	V	Nm
2250	63	0.80	0.988	186.41	117.75	136.14	0.50
2250	76	1.30	0.982	308.04	235.50	139.38	1.00
2250	82	1.80	0.975	433.33	353.25	142.50	1.50
2250	85	2.27	0.964	552.76	471.00	145.81	2.00
2250	87	2.73	0.955	673.17	588.75	149.01	2.50
2250	88	3.25	0.941	806.43	706.50	152.17	3.00
2250	89	3.70	0.927	929.76	824.25	156.58	3.50
2250	90	4.08	0.935	1050.58	942.00	159.00	4.00

Speed	**Efficiency**	**Current**	**Power factor**	**Input power**	**Output power**	**Output Voltage**	**Torque**
rpm	**%**	A	Cos φ	W	W	V	Nm
2500	61	0.83	0.991	213.59	130.83	149.98	0.50
2500	75	1.34	0.965	349.27	261.67	155.98	1.00
2500	81	1.84	0.956	485.37	392.50	159.30	1.50
2500	86	2.23	0.972	606.46	523.33	161.54	2.00
2500	86	2.82	0.941	761.05	654.17	165.63	2.50
2500	89	3.20	0.946	877.45	785.00	167.36	3.00

2500	89	3.65	0.938	1023.85	915.83	172.60	3.50
2500	89	4.08	0.930	1169.83	1046.67	178.00	4.00

Speed	Efficiency	Current	Power factor	Input power	Output power	Output Voltage	Torque
rpm	**%**	A	Cos φ	W	W	V	Nm
2750	59	0.86	0.982	243.48	143.92	166.48	0.50
2750	74	1.35	0.976	386.98	287.83	169.61	1.00
2750	80	1.85	0.970	539.41	431.75	173.46	1.50
2750	84	2.31	0.961	683.21	575.67	177.76	2.00
2750	86	2.78	0.953	832.18	719.58	181.26	2.50
2750	87	3.27	0.944	993.38	863.50	185.86	3.00
2750	88	3.75	0.924	1141.71	1007.42	190.16	3.50
2750	89	4.10	0.930	1287.84	1151.33	195.00	4.00

Speed	Efficiency	Current	Power factor	Input power	Output power	Output Voltage	Torque
rpm	**%**	A	Cos φ	W	W	V	Nm
3000	57	0.90	0.979	275.86	157.00	180.84	0.50
3000	72	1.40	0.967	434.39	314.00	185.16	1.00
3000	79	1.90	0.958	598.80	471.00	189.87	1.50
3000	83	2.35	0.967	760.82	628.00	193.27	2.00
3000	85	2.83	0.954	923.59	785.00	197.53	2.50
3000	87	3.32	0.935	1087.76	942.00	202.39	3.00

3000	88	3.76	0.923	1250.96	1099.00	208.08	3.50
3000	89	4.15	0.925	1409.57	1256.00	212.00	4.00

Table 7.2 Simulation analysis values

Simulation results							
Speed	**Efficiency**	**Current**	**Power factor**	**Input power**	**Output power**	**Output Voltage**	**Torque**
rpm	%	A	Cos φ	W	W	V	Nm
250	69.48	0.6843	0.9997	16.9423	12.8671	16.6957	0.50
	80.81	1.2453	0.9992	30.7513	25.7343	16.9302	1.00
	83.74	1.8055	0.9983	45.1102	38.6014	17.1624	1.50
	84.39	2.3538	0.9972	59.809	51.305	17.3866	2.00
	84.34	2.9013	0.9959	75.2007	64.1721	17.603	2.50
	83.71	3.4059	0.9945	90.8737	77.0394	17.8118	3.00
	82.79	3.9567	0.9927	107.154	89.743	18.0285	3.50
	81.65	4.5217	0.9909	124.2452	102.6104	18.2517	4.00
Speed	**Efficiency**	**Current**	**Power factor**	**Input power**	**Output power**	**Output Voltage**	**Torque**
rpm	%	A	Cos φ	W	W	V	Nm
500	71.67	0.6855	0.9996	33.905	26.1313	31.1929	0.50
	82.75	1.2465	0.9991	60.9989	52.2627	31.3678	1.00
	86.43	1.8075	0.9982	88.6644	78.3938	31.541	1.50
	87.75	2.358	0.9969	116.45	104.1164	31.705	2.00
	88.38	2.9127	0.9954	145.2223	130.2471	31.8597	2.50

	88.42	3.4107	0.9936	174.2273	156.379	32.0061	3.00
	88.27	3.9615	0.9915	203.652	182.1016	32.1548	3.50
	87.98	4.5229	0.9892	234.1199	208.2324	32.3066	4.00
Speed	**Efficiency**	**Current**	**Power factor**	**Input power**	**Output power**	**Output Voltage**	**Torque**
rpm	%	A	Cos φ	W	W	V	Nm
750	71.37	0.6856	0.9996	50.8243	39.3955	45.1988	0.50
	82.82	1.2466	0.9991	91.2074	78.7911	45.3195	1.00
	86.87	1.8077	0.9981	132.1836	118.1864	45.4373	1.50
	88.74	2.3584	0.9968	173.056	156.9275	45.545	2.00
	89.63	2.9138	0.9952	215.1853	196.3229	45.6422	2.50
	90.04	3.4112	0.9933	257.5569	235.7191	45.7305	3.00
	90.15	3.962	0.991	300.1294	274.4602	45.816	3.50
	90.05	4.523	0.9885	344.0031	313.8556	45.8995	4.00
Speed	**Efficiency**	**Current**	**Power factor**	**Input power**	**Output power**	**Output Voltage**	**Torque**
rpm	%	A	Cos φ	W	W	V	Nm
1000	70.58	0.6856	0.9996	68.325	52.3147	61.0768	0.50

	82.29	1.2467	0.9991	121.663	104.6294	61.1385	1.00
	86.72	1.8077	0.9981	175.6244	156.9436	61.1952	1.50
	88.84	2.3585	0.9967	229.2631	208.358	61.2407	2.00
	89.97	2.9139	0.9951	284.4333	260.6731	61.2748	2.50
	90.59	3.4112	0.9931	339.8652	312.9882	61.2993	3.00
	90.84	3.962	0.9908	395.2791	364.4028	61.3151	3.50
	90.95	4.523	0.9882	452.2567	416.7179	61.3234	4.00

Speed	**Efficiency**	**Current**	**Power factor**	**Input power**	**Output power**	**Output Voltage**	**Torque**
rpm	%	A	Cos φ	W	W	V	Nm
1250	69.77	0.6856	0.9996	86.3073	65.579	75.8205	0.50
	81.76	1.2467	0.9991	152.9477	131.1577	75.8296	1.00
	86.43	1.8077	0.9981	220.2425	196.7365	75.8305	1.50
	88.75	2.3585	0.9967	287.0003	261.1704	75.8195	2.00
	90.06	2.9139	0.995	355.564	326.749	75.7961	2.50
	90.79	3.4112	0.9931	424.4096	392.3288	75.7624	3.00
	91.21	3.962	0.9907	493.0171	456.7627	75.7149	3.50
	91.43	4.523	0.988	563.4499	522.3418	75.6552	4.00

Speed	Efficiency	Current	Power factor	Input power	Output power	Output Voltage	Torque
rpm	%	A	Cos φ	W	W	V	Nm
1500	68.56	0.6856	0.9996	104.5996	78.8432	90.4024	0.50
	80.8	1.2467	0.9991	184.5435	157.6866	90.3586	1.00
	85.81	1.8077	0.9981	265.1766	236.5293	90.3051	1.50
	88.39	2.3585	0.9967	345.0591	313.9817	90.2389	2.00
	89.86	2.9139	0.995	427.0245	392.8248	90.1593	2.50
	90.75	3.4112	0.9931	509.2933	471.6696	90.0691	3.00
	91.25	3.962	0.9907	591.0506	549.1219	89.7885	3.50
	91.53	4.523	0.988	674.8698	627.965	89.4197	4.00

Speed	Efficiency	Current	Power factor	Input power	Output power	Output Voltage	Torque
rpm	%	A	Cos φ	W	W	V	Nm
1750	67.02	0.6939	0.9996	124.6154	92.1073	106.6479	0.50
	79.88	1.2467	0.9991	217.8535	184.2145	106.5509	1.00
	85.17	1.8077	0.9981	311.8322	276.3213	106.4385	1.50
	87.88	2.3585	0.9967	404.8543	366.7919	106.3107	2.00

	89.45	2.9139	0.995	500.2402	458.8997	106.169	2.50
	90.51	3.4112	0.9931	595.9496	551.0083	106.0101	3.00
	91.12	3.962	0.9907	690.8258	641.4795	105.5401	3.50
	91.48	4.523	0.9879	787.9588	733.5867	105.3026	4.00

Speed	Efficiency	Current	Power factor	Input power	Output power	Output Voltage	Torque
rpm	%	A	Cos φ	W	W	V	Nm
2000	65.7	0.7516	0.9996	143.6919	105.0267	120.5969	0.50
	78.94	1.2896	0.999	249.919	210.053	120.4495	1.00
	84.52	1.8137	0.9981	356.8104	315.0791	120.2912	1.50
	87.34	2.3585	0.9967	462.5778	418.2243	120.1157	2.00
	89.1	2.9139	0.9951	571.019	523.2509	119.9205	2.50
	90.2	3.4112	0.9931	679.8029	628.279	119.7067	3.00
	90.91	3.962	0.9907	787.6703	731.4235	119.4152	3.50
	91.41	4.523	0.9879	898.1536	836.45	119.1351	4.00

Speed	Efficiency	Current	Power factor	Input power	Output power	Output Voltage	Torque
rpm	%	A	Cos φ	W	W	V	Nm

2250	64.01	0.7544	0.9996	164.1135	118.2906	135.8238	0.50
	77.64	1.3117	0.999	283.7101	236.5819	135.6179	1.00
	83.59	1.8551	0.998	404.0442	354.8718	135.3735	1.50
	86.67	2.3653	0.9967	522.7565	471.0355	134.8313	2.00
	88.54	2.9139	0.995	644.4651	589.326	134.2644	2.50
	89.78	3.4112	0.9931	766.5797	707.6192	133.7135	3.00
	90.58	3.962	0.9906	887.6629	823.7829	133.4028	3.50
	91.14	4.5299	0.9878	1011.6938	942.0732	133.0644	4.00
Speed	**Efficiency**	**Current**	**Power factor**	**Input power**	**Output power**	**Output Voltage**	**Torque**
rpm	%	A	Cos φ	W	W	V	Nm
2500	62.51	0.7549	0.9996	186.8089	131.5553	151.6039	0.50
	76.54	1.3159	0.999	319.7312	263.11	151.3411	1.00
	82.7	1.8764	0.998	453.4873	394.6645	151.0146	1.50
	85.88	2.4247	0.9966	585.6044	523.8469	150.5893	2.00
	87.97	2.9696	0.9949	720.8572	655.4021	150.1429	2.50
	89.33	3.4711	0.9929	856.5859	786.9595	149.7216	3.00
	90.23	4.0219	0.9905	990.967	916.1419	149.3444	3.50

Speed	Efficiency	Current	Power factor	Input power	Output power	Output Voltage	Torque
	90.87	4.5892	0.9876	1128.5194	1047.6955	148.9383	4.00

Speed	Efficiency	Current	Power factor	Input power	Output power	Output Voltage	Torque
rpm	%	A	Cos φ	W	W	V	Nm
2750	60.81	0.7491	0.965	208.0394	144.4744	164.921	0.50
	75.23	1.3096	0.9796	353.9336	288.9486	164.542	1.00
	81.7	1.8681	0.9861	500.6734	433.4222	164.048	1.50
	85.18	2.4162	0.9886	645.5876	575.2787	163.4693	2.00
	87.35	2.9287	0.9896	793.7621	719.753	162.8576	2.50
	88.8	3.4656	0.9896	942.8242	864.2297	162.2259	3.00
	89.77	4.0131	0.9889	1090.0649	1006.087	161.5646	3.50
	90.49	4.5737	0.9879	1240.7346	1150.563	160.8336	4.00

Speed	Efficiency	Current	Power factor	Input power	Output power	Output Voltage	Torque
rpm	%	A	Cos φ	W	W	V	Nm
3000	58.83	0.5423	0.5664	233.8025	157.7383	171.5203	0.50
	73.62	1.0783	0.6807	393.4906	315.4775	170.6604	1.00
	80.43	1.6055	0.7579	553.9491	473.2149	169.7842	1.50

	84.12	2.1139	0.8113	712.3031	628.0901	168.7908	2.00
	86.42	2.6305	0.8521	874.3779	785.8283	167.7663	2.50
	87.99	3.1339	0.9053	1035.8743	943.5699	166.5104	3.00
	89.14	3.6502	0.9506	1194.834	1098.4445	165.2223	3.50
	90.13	4.1888	0.9667	1358.222	1256.1851	163.9891	4.00